Article

Mitochondrial chaperone HSP-60 regulates anti-bacterial immunity via p38 MAP kinase signaling

Dae-Eun Jeong[1,†], Dongyeop Lee[1,†], Sun-Young Hwang[1,‡], Yujin Lee[1], Jee-Eun Lee[1], Mihwa Seo[2], Wooseon Hwang[1], Keunhee Seo[1], Ara B Hwang[1,§], Murat Artan[3], Heehwa G Son[1], Jay-Hyun Jo[1,¶], Haeshim Baek[1], Young Min Oh[1,††], Youngjae Ryu[4], Hyung-Jun Kim[4], Chang Man Ha[4], Joo-Yeon Yoo[1,*] (iD) & Seung-Jae V Lee[1,2,3,**] (iD)

Abstract

Mitochondria play key roles in cellular immunity. How mitochondria contribute to organismal immunity remains poorly understood. Here, we show that HSP-60/HSPD1, a major mitochondrial chaperone, boosts anti-bacterial immunity through the up-regulation of p38 MAP kinase signaling. We first identify 16 evolutionarily conserved mitochondrial components that affect the immunity of *Caenorhabditis elegans* against pathogenic *Pseudomonas aeruginosa* (PA14). Among them, the mitochondrial chaperone HSP-60 is necessary and sufficient to increase resistance to PA14. We show that HSP-60 in the intestine and neurons is crucial for the resistance to PA14. We then find that p38 MAP kinase signaling, an evolutionarily conserved anti-bacterial immune pathway, is down-regulated by genetic inhibition of *hsp-60*, and up-regulated by increased expression of *hsp-60*. Overexpression of *HSPD1*, the mammalian ortholog of *hsp-60*, increases p38 MAP kinase activity in human cells, suggesting an evolutionarily conserved mechanism. Further, cytosol-localized HSP-60 physically binds and stabilizes SEK-1/MAP kinase kinase 3, which in turn up-regulates p38 MAP kinase and increases immunity. Our study suggests that mitochondrial chaperones protect host eukaryotes from pathogenic bacteria by up-regulating cytosolic p38 MAPK signaling.

Introduction

Emerging evidence indicates that mitochondria play key roles in anti-viral and anti-bacterial innate immunity in mammalian cells (West *et al*, 2011). For example, mitochondria protect cells from pathogens by the generation of reactive oxygen species (ROS) that eliminate bacteria. Mitochondria also provide a membrane platform on which pathogen-responsive immune effector proteins boost inflammatory signals. However, mechanisms by which mitochondria modulate immunity remain largely unknown, in particular, at the organism level.

Caenorhabditis elegans has been used as an excellent model to study organismal innate immunity against pathogenic microbes (Ewbank, 2006; Irazoqui *et al*, 2010; Kim & Ewbank, 2015; Ewbank & Pujol, 2016). Previous studies have identified important immune regulators against bacterial pathogens; these include PMK-1/p38 mitogen-activated protein kinase (p38 MAPK) (Kim *et al*, 2002), and transcription factors, SKN-1 (Papp *et al*, 2012), ZIP-2 (Estes *et al*, 2010), and DAF-16/FOXO (Garsin *et al*, 2003; Evans *et al*, 2008). Among them, PMK-1 is essential for resistance against infection by various pathogenic bacteria, including *Pseudomonas aeruginosa* (Kim *et al*, 2002, 2004; Troemel *et al*, 2006; Powell *et al*, 2009; Ren *et al*, 2009; Shivers *et al*, 2009, 2010; Bolz *et al*, 2010; Richardson *et al*, 2010; Pukkila-Worley & Ausubel, 2012; Kim, 2013). PMK-1 is activated via phosphorylation by the upstream kinase cascade, composed of SEK-1/MKK3 (MAPK kinase) and NSY-1/ASK1 (MAPK kinase kinase), which also mediate immunity against pathogenic bacteria. The activation of the PMK-1 signaling cascade by *P. aeruginosa* infection is dependent on Toll-interleukin-1 receptor (TIR)

1   Department of Life Sciences, Pohang University of Science and Technology, Pohang, Gyeongbuk, Korea
2   School of Interdisciplinary Bioscience and Bioengineering, Pohang University of Science and Technology, Pohang, Gyeongbuk, Korea
3   Information Technology Convergence Engineering, Pohang University of Science and Technology, Pohang, Gyeongbuk, Korea
4   Research Division, Korea Brain Research Institute, Daegu, Korea
    *Corresponding author. Tel: +82 54 279 2346; E-mail: jyoo@postech.ac.kr
    **Corresponding author. Tel: +82 54 279 2351; E-mail: seungjaelee@postech.ac.kr
    †These authors contributed equally to this work
    ‡Present address: Program in Molecular, Cell and Cancer Biology, University of Massachusetts Medical School, Worcester, MA, USA
    §Present address: Department of Orthopaedic Surgery, Eli and Edythe Broad Center of Regeneration Medicine and Stem Cell Research, University of California, San Francisco, San Francisco, CA, USA
    ¶Present address: Dermatology Branch, Center for Cancer Research, National Cancer Institute, National Institutes of Health, Bethesda, MD, USA
    ††Present address: Bio Research Institute, Genexine Inc., Korea Bio Park, Seongnam, Gyeonggi-do, Korea

domain-containing protein TIR-1/SARM (Couillault *et al*, 2004; Liberati *et al*, 2004).

Mitochondria also play roles in the resistance of *C. elegans* against pathogenic bacteria by regulating ROS production, mitophagy, and mitochondrial unfolded protein response (UPR^{MT}) (Hwang *et al*, 2014; Liu *et al*, 2014; Pellegrino *et al*, 2014; Kirienko *et al*, 2015; Ewbank & Pujol, 2016). Under stress conditions, UPR^{MT} sends signals to the nucleus through HAF-1, a mitochondrial peptide exporter (Haynes *et al*, 2010), and up-regulates transcription factors including ATFS-1 (Haynes *et al*, 2010), DVE-1 (Haynes *et al*, 2007), its cofactor UBL-5 (Benedetti *et al*, 2006), and chromatin remodeling factors (Merkwirth *et al*, 2016; Tian *et al*, 2016). This leads to the induction of genes such as mitochondrial chaperones, which help alleviate perturbed protein homeostasis in mitochondria (Pellegrino *et al*, 2013). UPR^{MT} also increases the expression of several anti-microbial genes in *C. elegans* in an ATFS-1-dependent manner, and contributes to anti-bacterial immunity (Nargund *et al*, 2012; Pellegrino *et al*, 2014). In addition, inhibition of mitochondrial complex I up-regulates PMK-1 signaling (Chikka *et al*, 2016). Despite these advances, the link between mitochondrial factors and immune signaling pathways in *C. elegans* remains elusive.

In this study, we aim to identify evolutionarily conserved mitochondrial factors that contribute to organismal immunity using *C. elegans* and *P. aeruginosa* as the host and pathogen, respectively. We find that the mitochondrial chaperone HSP-60 enhances *C. elegans* immunity against *P. aeruginosa*. We demonstrate that HSP-60 in the intestine and neurons is crucial for the resistance to PA14. We then show that HSP-60 up-regulates the PMK-1 signaling pathway, which confers the increased immunity. Using cultured human cells, we find that the activity of p38 MAPK is increased by HSPD1, the ortholog of HSP-60. Furthermore, we show that a fraction of HSP-60 in the cytosol increases the PA14 immunity by binding and stabilizing SEK-1/MKK3, which up-regulates p38 MAP kinase. Our study raises the possibility that mitochondrial chaperones protect hosts from pathogens by the up-regulation of cytosolic PMK-1/p38 MAPK signaling, which is an evolutionarily conserved immune process.

Results

A genetic screen identifies mitochondrial components that regulate *Caenorhabditis elegans* immunity

We sought to identify mitochondrial factors that were critical for immunity using *C. elegans* as the host animal and PA14 as the pathogenic bacteria. We specifically focused on evolutionarily conserved nuclear-encoded mitochondrial components because of their potential implication in mammalian immunity (Appendix Fig S1A; also see Materials and Methods). We knocked down 220 such mitochondrial components with available RNAi clones and measured the survival of *C. elegans* fed on PA14 by using a standard infection ("slow killing") assay (Appendix Fig S1A) (Tan *et al*, 1999). As potential immune-regulatory genes, we identified 16 RNAi clones that reproducibly increased or decreased the survival of animals following PA14 infection (arbitrary cutoff: ±10% change in mean survival, and *P*-value < 0.001, Fig 1A and Table 1).

We classified these 16 genes based on the effects of their RNAi knockdown on known immune-regulatory signaling pathways against PA14 infection, including PMK-1/p38 MAPK (Kim *et al*, 2002), and the three transcription factors, ZIP-2 (Estes *et al*, 2010), SKN-1/Nrf (Papp *et al*, 2012), and DAF-16/FOXO (Garsin *et al*, 2003; Evans *et al*, 2008) (Fig 1B–D and Appendix Fig S1A). We measured the survival of *pmk-1*, *zip-2*, and *daf-16* mutants after PA14 infection upon treatment with each of the 16 RNAi clones (Fig 1B). We also examined the effects of the RNAi clones on downstream target gene GFP reporters for these regulators, including *T24B8.5* for PMK-1 (Shivers *et al*, 2009), *irg-1* for ZIP-2 (Estes *et al*, 2010), *gst-4* for SKN-1 (Kahn *et al*, 2008), and *sod-3* for DAF-16 (Honda & Honda, 1999; Libina *et al*, 2003) (Fig 1C). We analyzed the results using a heat map, which exhibited three clusters (Fig 1B–D and Appendix Fig S1B; see Appendix Fig S1 legend for the detailed description of these clusters). RNAi knockdown of the cluster I genes decreased the survival of worms following PA14 infection in a *pmk-1*-dependent manner as well as the expression levels of the PMK-1 reporter, *T24B8.5p::GFP* (Fig 1B and C). The RNAi clones targeting cluster II genes tended to decrease the survival of worms infected with PA14 in a *zip-2*-dependent manner (Fig 1B). Knockdown of many cluster III genes, which are implicated in mitochondrial mRNA translation and respiration, increased the survival of animals following PA14 infection partly in *zip-2*- and *daf-16*-dependent manners (Fig 1B). The cluster III RNAi clones also generally decreased the induction of *irg-1p::GFP*, but increased the expression of the *gst-4p::GFP* upon PA14 infection (Fig 1C). Overall, the mitochondrial components in these three different clusters appear to influence PA14 susceptibility by acting through different immune regulators.

The mitochondrial chaperone HSP-60 in the intestine and neurons is required for immunity against *Pseudomonas aeruginosa*

We found that the knockdown of the *hsp-60* had the most robust effect on PA14 resistance, which was up to a 43% decrease (Table 1 and Fig 2A). The accumulation of GFP-labeled PA14 in the intestinal lumen was also increased by *hsp-60* RNAi (Fig 2B and C). This result indicates that *hsp-60* is required for the clearance of PA14. In contrast, *hsp-60* RNAi did not affect the avoidance behavior of worms to PA14 (Fig 2D–F). *hsp-60* RNAi also had little effect on the lifespan of the worms following standard *Escherichia coli* (*E. coli*) diet feeding (Fig 2G), or on the survival upon pathogenic *Enterococcus faecalis* (*E. faecalis*) or pathogenic *E. coli* infection (Fig 2H and I). Together, these data suggest that HSP-60 is specifically required for resistance to PA14 infection by affecting intrinsic immunity, without altering lifespan or behavioral responses to pathogens.

Next, we determined in which tissues HSP-60 was required for the resistance to PA14. By performing tissue-specific RNAi experiments (Qadota *et al*, 2007; Calixto *et al*, 2010), we found that intestine- or neuron-specific *hsp-60* knockdown robustly increased the susceptibility of animals to PA14 (Fig 3A and B). In contrast, treatment with *hsp-60* RNAi specifically in the hypodermis, muscle, or in control animals did not influence survival upon PA14 infection (Fig 3C–F). Thus, HSP-60 expression in the intestine and neurons contributes to the anti-PA14 immunity.
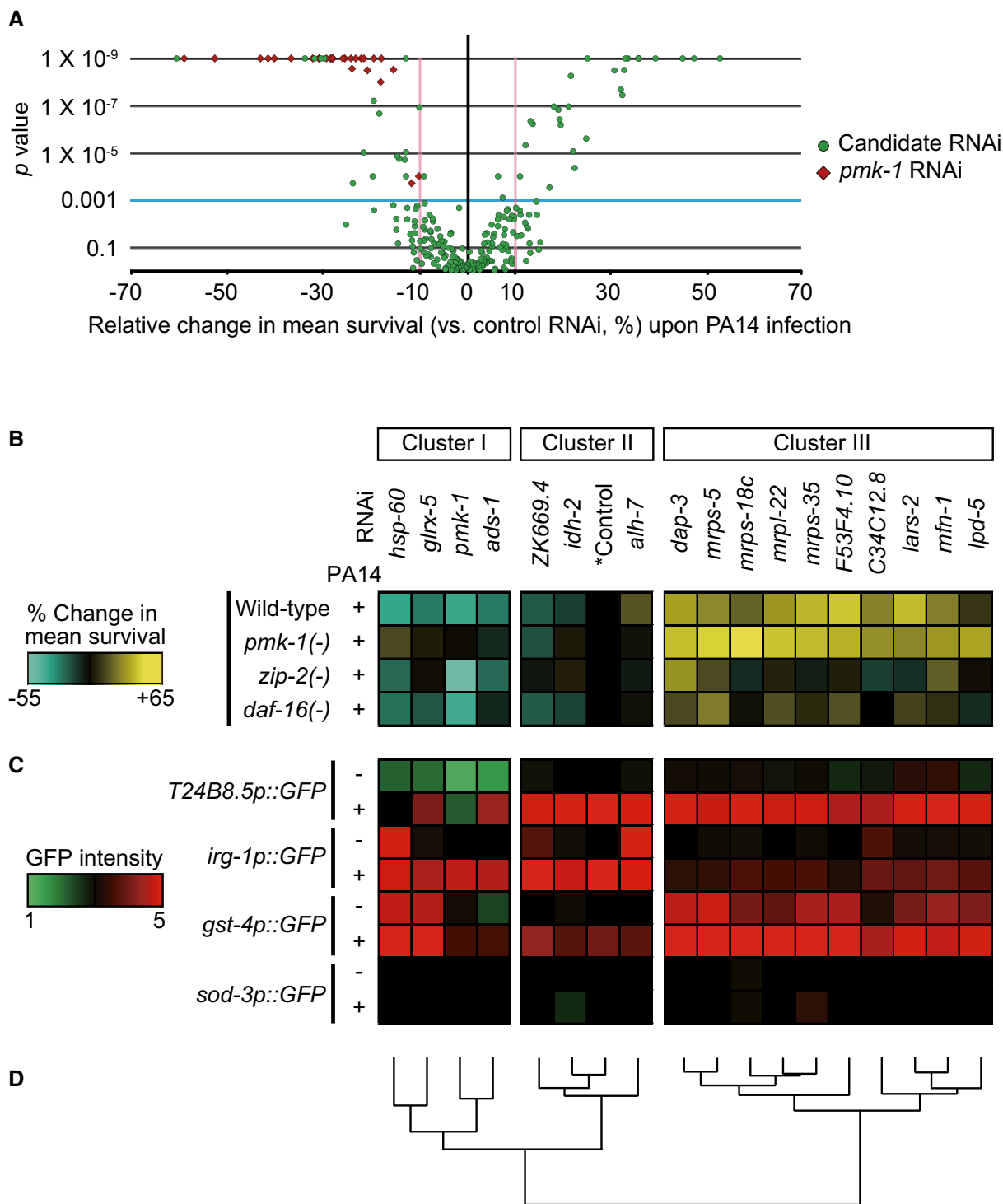
Figure 1. Targeted RNAi screen for mitochondrial components that affect anti-PA14 immunity in *Caenorhabditis elegans*.

A   A volcano plot exhibits mean survival changes and *P*-values on PA14 after pre-treatment with each of RNAi clones targeting evolutionarily conserved mitochondrial components. *P*-values were calculated by using log-rank test. *pmk-1* RNAi (red diamond) was used as a positive control.

B, C   Heat maps were generated based on the effects of RNAi clones on the survival of animals in different genetic backgrounds upon PA14 infection (average values of % changes in mean survival obtained from two independent trials) (B) and on the expression levels of GFP reporters for known immune effector proteins (C). Asterisk indicates effects by empty vector controls.

D   Genes in the heat maps shown in panels (B) and (C) were randomly clustered into three groups (clusters I, II, and III) by using Cluster 3.0.

Data information: See Datasets EV1 and EV2, and Appendix Table S1 for the filtering processes of our gene list, statistical analysis for the survival data and semi-quantitative analysis of GFP reporters shown in this figure.

Table 1. List of mitochondrial genes whose knockdown reproducibly influences the survival of *Caenorhabditis elegans* on PA14.

Gene			% Change in mean survival	
Human	*C. elegans*	Description	RNAi screen	2nd repeat
HSPD1	*hsp-60*	Mitochondria-specific chaperone	−31.9	−36.9
AGP5	*ads-1*	Alkyldihydroxyacetonephosphate synthase, peroxisomal	−29.9	−26.0
GLRX5	*glrx-5*	Glutaredoxin-related protein 5 (mitochondrial), involved in the biogenesis of iron–sulfur clusters and normal iron homeostasis	−19.4	−25.9
DBT	*ZK669.4*	Dihydrolipoamide branched chain transacylase	−30.6	−18.8
IDH2	*idh-2*	Mitochondria isocitrate dehydrogenase	−60.6	−12.4
NDUFS4	*lpd-5*	An accessory subunit of the mitochondrial membrane respiratory chain NADH dehydrogenase (complex I), or NADH	22.1	10.2
ALDH5A1	*alh-7*	Aldehyde dehydrogenase	32.5	16.7
NDUFV2	*F53F4.10*	NADH dehydrogenase [ubiquinone] flavoprotein 2	22.5	20.6
GRPEL1	*C34C12.8*	GrpE protein homolog 1, Hsp70 cochaperone	35.4	26.8
LARS2	*lars-2*	Leucyl amino-acyl tRNA synthetase	17.9	27.9
MRPS5	*mrps-5*	Mitochondrial ribosomal protein	30	29.0
MRPL3	*mrps-18C*	Mitochondrial ribosomal protein	34.1	32.0
DAP3	*dap-3*	Death-associated protein 3, mitochondrial ribosomal protein that promotes apoptosis	47.0	34.5
MRPL22	*mrpl-22*	Mitochondrial ribosomal protein	24.6	39.8
SLC25A37	*mfn-1*	Mitoferrin, iron importer for the synthesis of mitochondrial heme and iron–sulfur clusters	32.0	41.0
MRPS35	*mrps-35*	Mitochondrial ribosomal protein	32.1	43.2

The mitochondrial unfolded protein response is required for the resistance of *Caenorhabditis elegans* against PA14

We tested whether the PA14 susceptibility was affected by knockdown of UPR^{MT} components other than HSP-60, including DVE-1 (Haynes *et al*, 2007), UBL-5 (Benedetti *et al*, 2006), and ATFS-1, and the mitochondrial peptide exporter HAF-1 (Haynes *et al*, 2010). We found that the genetic inhibition of *dve-1* or *ubl-5* significantly increased susceptibility to PA14 (Fig EV1A and B). Mutations in *atfs-1* increased susceptibility to PA14 as well (Fig EV1C), as shown previously (Pellegrino *et al*, 2014). Our data are consistent with the findings that these factors transcriptionally up-regulate HSP-60 (Benedetti *et al*, 2006; Haynes *et al*, 2007, 2010). In contrast, the *haf-1* mutation did not affect the survival following PA14 infection (Fig EV1D). Thus, HAF-1 might not participate in the resistance to PA14, although the result can be interpreted with different reasons such as redundancy. Together, these data indicate that UPR^{MT}, in general, is required for the PA14 resistance.

HSP-60 regulates immunity against PA14 via PMK-1 signaling pathway

We examined whether UPR^{MT} components affected the activity of known immunity factors. Consistent with our heat map data (Fig 1C), *hsp-60* RNAi decreased the induction of the *T24B8.5p::GFP*, a PMK-1 activity reporter, upon PA14 infection (Fig 4A and B). Knockdown of *dve-1* or *ubl-5* also suppressed the PA14-induced *T24B8.5p::GFP* (Fig EV2A and B). In addition, *hsp-60* RNAi reduced the levels of *F35E12.5p::GFP*, another PMK-1 reporter (Fig EV2C and D) (Bolz *et al*, 2010), and three selected PMK-1-regulated target

mRNAs (*T24B8.5*, *C17H12.8* and *K08D8.5*) (Shivers *et al*, 2010) following PA14 infection (Fig 4C–E). Further, knockdown of *hsp-60* reduced the level of active phospho-PMK-1 under both control and PA14-infected conditions (Figs 4F and EV2G). These data indicate that *hsp-60* is required for maintaining the basal levels of active PMK-1. Consistently, knockdown of *hsp-60* did not further reduce the survival of *pmk-1* mutants following infection with PA14 (Fig 4G), but robustly decreased the survival of *zip-2* and *daf-16* mutants (Fig 4H and I). Together, these data suggest that HSP-60 contributes to the resistance against PA14 by up-regulating PMK-1.

TIR-1/SARM is a positive upstream regulator of PMK-1 signaling (Liberati *et al*, 2004), and gain-of-function (*gf*) mutations of *tir-1/SARM* increase anti-PA14 immunity (Xie *et al*, 2013). We found that *hsp-60* RNAi suppressed the induction of *T24B8.5p::GFP* conferred by *tir-1(gf)* mutations (Fig 5A and B). In addition, enhanced PA14 resistance conferred by *tir-1(gf)* mutations was largely suppressed by *hsp-60* RNAi (Fig 5C). These data indicate that HSP-60 may act downstream of or in parallel with TIR-1 to regulate PMK-1 activity and immunity against PA14.

Increased expression of HSP-60 is sufficient for enhancing immunity

We then asked whether increased expression of *hsp-60* affected anti-PA14 immunity by generating transgenic worms that expressed *hsp-60* with or without a GFP tag (*hsp-60::GFP Tg* or *hsp-60 Tg*). We first confirmed that these transgenes increased the levels of *hsp-60* mRNA (Fig EV3A and D) and HSP-60::GFP protein (Fig EV3B and C). We then showed that the GFP-fused HSP-60 was mainly localized to the mitochondria of cells in multiple tissues (Fig 6A–F; but
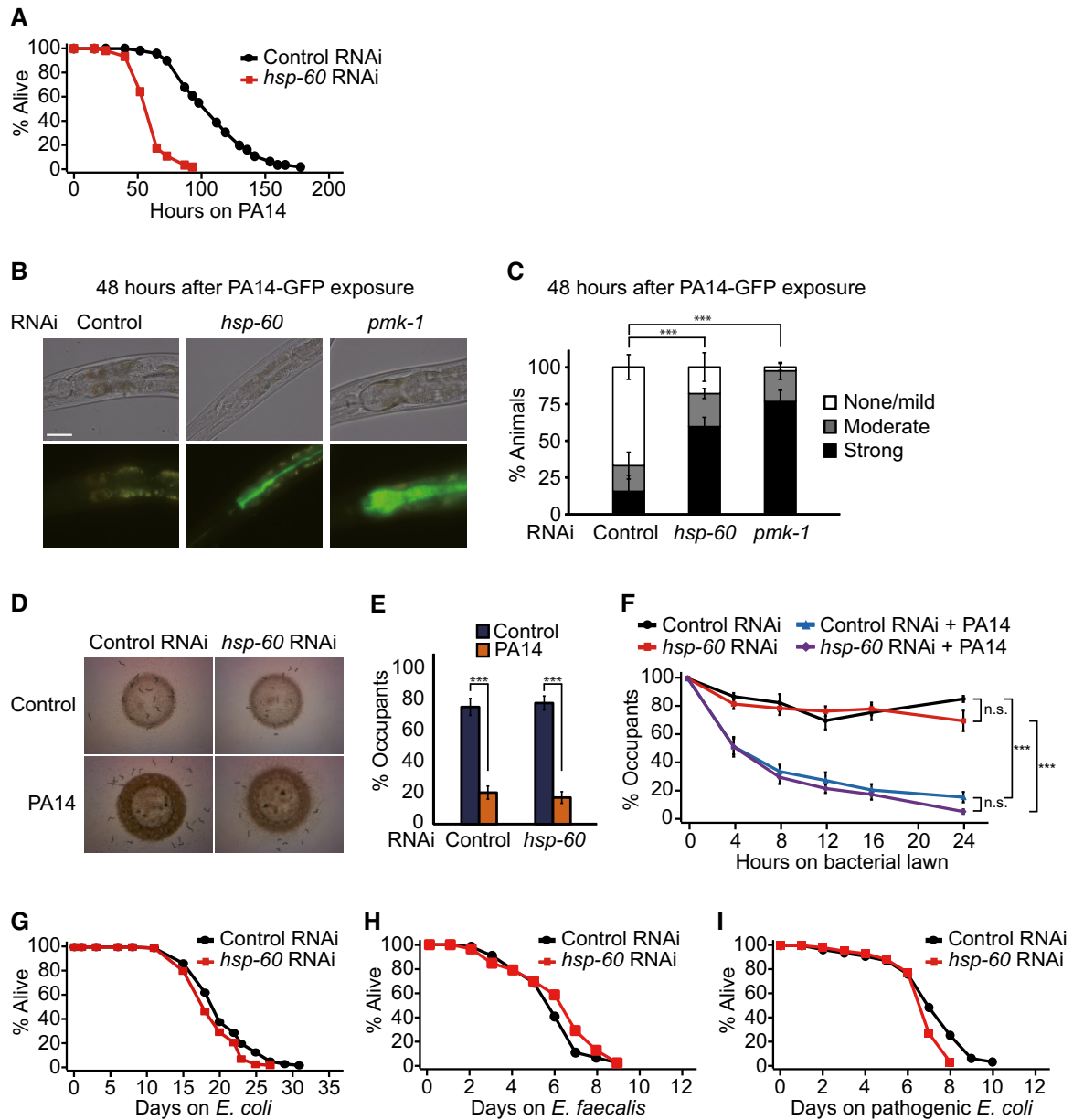
Figure 2. HSP-60 is required for resistance against PA14 in *Caenorhabditis elegans*.

A   RNAi knockdown of *hsp-60* decreased the survival of animals on PA14. See Appendix Fig S2A for results showing that *hsp-60* RNAi reduced survival on PA14 without 5-fluoro-2′-deoxyuridine (FUdR) treatment.

B   Shown are representative images of worms, which were pre-treated with control RNAi, *hsp-60* RNAi or *pmk-1* RNAi, after PA14-GFP exposure for 48 h. Scale bar indicates 40 μm.

C   Semi-quantification of PA14-GFP levels in panel (B) ($n \geq 23$ from three independent experiments). Error bars represent standard error of the mean (SEM). *P*-values were calculated by using chi-squared test (***$P < 0.001$). *pmk-1* RNAi, which increases the accumulation of PA14-GFP in the intestinal lumen (Kim *et al*, 2002), was used as a positive control.

D   Bacterial lawn occupancy of wild-type animals pre-treated with control or *hsp-60* RNAi upon *Escherichia coli* (HT115) or PA14 exposure for 16 h.

E   Quantification of data in panel (D) ($n \geq 100$ from three independent experiments). Error bars represent SEM. *P*-values were obtained by using two-tailed Student's *t*-test (***$P < 0.001$).

F   Time-course data of the PA14 avoidance assays indicate that worms treated with *hsp-60* RNAi did not display defects in PA14 avoidance ($n = 3$). Error bars represent SEM. *P*-values were calculated by two-way ANOVA test (***$P < 0.001$).

G   *hsp-60* RNAi had a small effect on the lifespan of animals on a normal *E. coli* (HT115) diet.

H, I   Knockdown of *hsp-60* had little or no effect on the survival of worms infected with *Enterococcus faecalis* without 5-fluoro-2′-deoxyuridine (FUdR) treatment (H) or pathogenic *E. coli* (I). *pmk-1* RNAi that decreases the survival of animals on both *E. faecalis* (Shivers *et al*, 2010) and pathogenic *E. coli* was used as a positive control (Appendix Fig S2B and C). See Appendix Fig S2D and E for data showing that treatment with *E. faecalis* or pathogenic *E. coli* did not induce mitochondrial chaperone genes *hsp-6* or *hsp-60*.

Data information: See Appendix Table S2 for additional repeats and statistical analysis for the survival and the lifespan data shown in this figure.
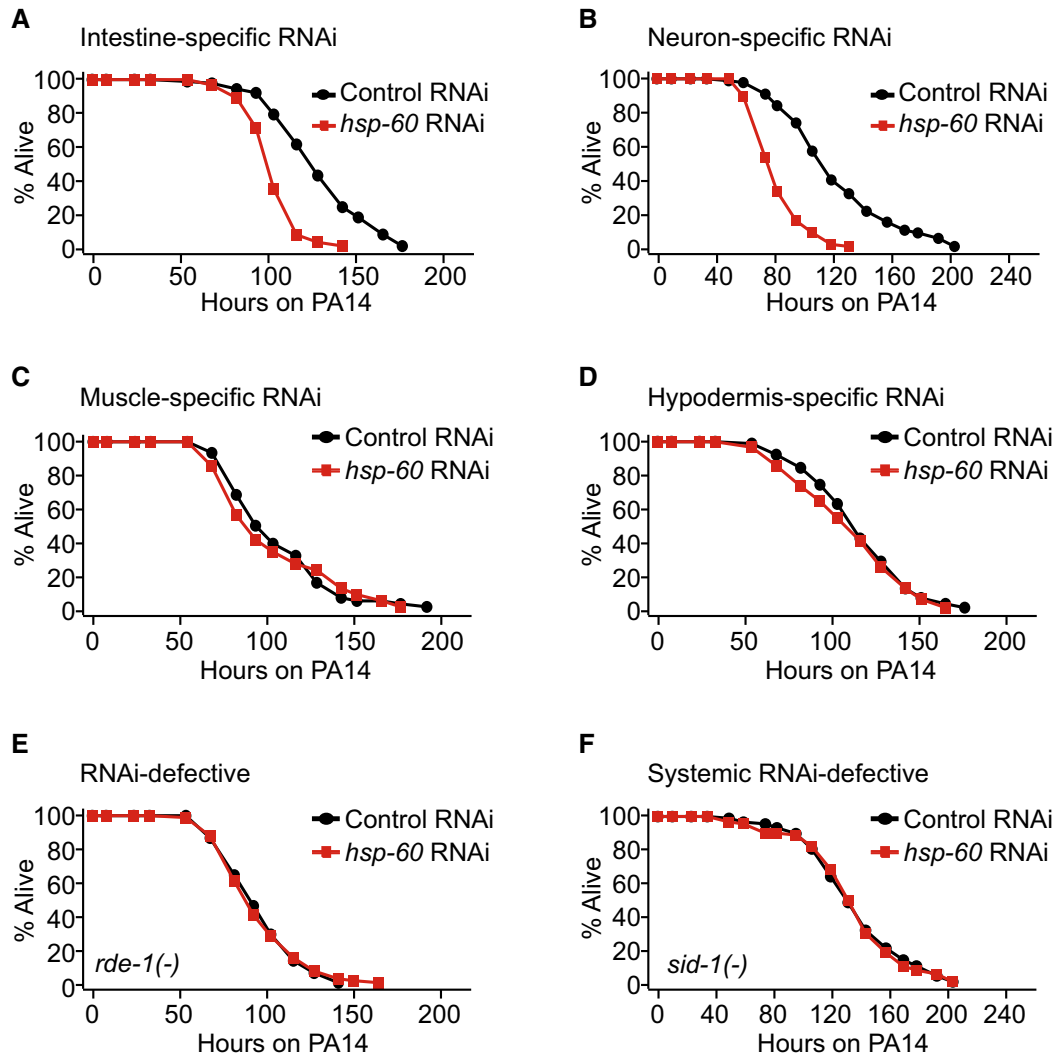
Figure 3. *hsp-60* in the intestine and neurons is required for anti-PA14 immunity.

A–D   Intestine (A)- or neuron (B)-specific *hsp-60* RNAi increased PA14 susceptibility, whereas muscle (C)- or hypodermis (D)-specific *hsp-60* RNAi did not. *rde-1(ne219)* mutant animals that expressed *rde-1* under the control of an intestine-specific *nhx-2* promoter, a muscle-specific *hlh-1* promoter or a hypodermis-specific *lin-26* promoter, and *sid-1* mutant animals that expressed *sid-1* driven by a neuron-specific *unc-119* promoter were used for tissue-specific RNAi experiments (Qadota *et al*, 2007; Calixto *et al*, 2010).

E, F   Upon PA14 infection, *hsp-60* RNAi did not affect the survival of RNAi-defective *rde-1(ne219)* (E) or systemic RNAi-defective *sid-1(pk3321)* (F) mutants.

Data information: See Appendix Table S3 for additional repeats and statistical analysis for survival and lifespan data shown in this figure.

see also Fig 9B and legends). Importantly, both *hsp-60::GFP Tg* and *hsp-60 Tg* significantly increased resistance to PA14 (Figs 6G, and EV3E and F), which was abolished by *hsp-60* RNAi (Fig 6H). The lifespan on a standard *E. coli* diet was not extended by *hsp-60::GFP Tg* (Figs 6I and EV3G), suggesting the specific role of *hsp-60* in survival upon PA14 infection.

As overexpression of exogenous proteins in subcellular organelles can result in stresses (Gibson *et al*, 2013), we considered the possibility that transgenic expression of *hsp-60* may have elicited mitochondrial unfolded protein response (UPR^{MT}) to increase immunity. Several lines of evidence argue against this possibility. First, overexpression of only GFP in mitochondria (GFP^{MT}) driven by *hsp-60* promoter with mitochondria-targeting sequence (MTS) of

hsp-60 (Appendix Fig S3A–C) did not increase the survival of animals on PA14 (Appendix Fig S3D). Second, *hsp-60::GFP* transgenes did not affect the expression of *hsp-6* (Appendix Fig S4A), another mitochondrial chaperone that is induced by UPR^{MT} (Yoneda *et al*, 2004). Third, *hsp-60::GFP* transgenes had little effect on development, whereas mitochondrial stresses caused by treatment with *spg-7/spastic paraplegia-7* RNAi or *cco-1/cytochrome C oxidase-1* RNAi, or with ethidium bromide (EtBr) substantially delayed the development (Appendix Fig S4B and C). *hsp-60::GFP Tg* animals displayed impaired reproduction, which is known to correlate with increased resistance against PA14 (Miyata *et al*, 2008). However, day 6 post-reproductive *hsp-60::GFP Tg* animals displayed increased survival on PA14, suggesting that *hsp-60::GFP* transgene-mediated
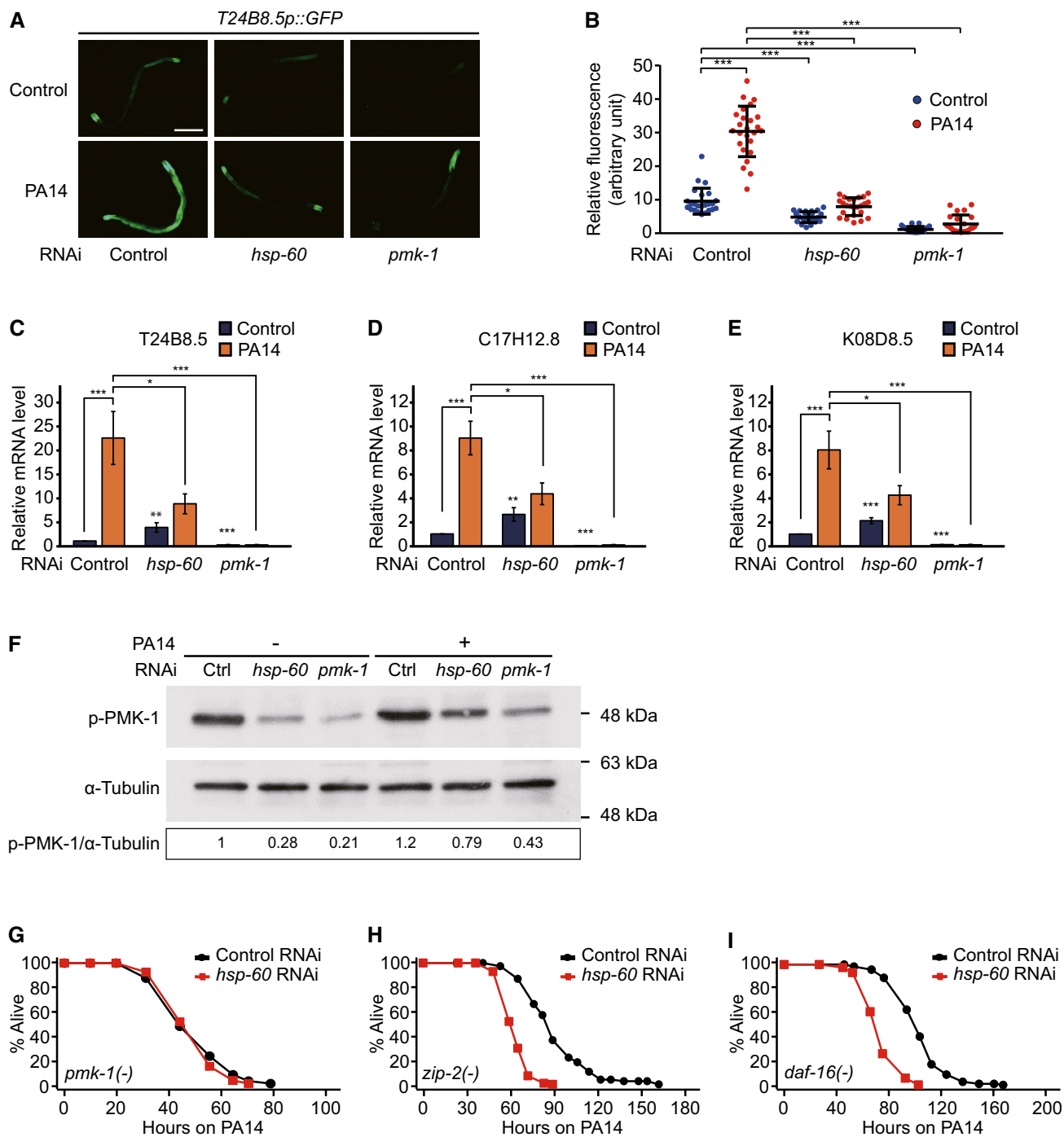
Figure 4. *hsp-60* **is required for maintaining the basal levels of PMK-1.**

A   *hsp-60* RNAi decreased the expression of *T24B8.5p::GFP*. Scale bar indicates 200 μm.

B   Quantification of data in panel (A) ($n \geq 23$). Note that the same data for control RNAi and *pmk-1* RNAi are also shown in Fig EV2A and B for comparison.

C–E   qRT–PCR analysis data that show mRNA levels of three selected PMK-1-regulated genes, *T24B8.5* (C), *C17H12.8* (D), and *K08D8.5* (E) upon knocking down *hsp-60* with or without PA14 treatment ($n \geq 7$).

F   Western blot assays showed that *hsp-60* RNAi decreased the level of phospho-PMK-1 (p-PMK-1) with or without PA14 treatment, which is comparable to *pmk-1* RNAi. The blot is a representative one from four repeats that showed consistent results. α-tubulin was used as a loading control. The numbers indicate relative intensities of the p-PMK-1 bands normalized to α-tubulin. See Fig EV2G for the quantification data.

G–I   Upon PA14 infection, *hsp-60* knockdown did not influence the survival of *pmk-1(km25)* mutants (G), but significantly decreased the survival of *zip-2(tm4067)* (H) and *daf-16(mu86)* mutants (I).

Data information: *pmk-1* RNAi was used as a positive control for panels (A–F). Error bars represent SEM. *P*-values were calculated by two-tailed Student's *t*-test (*$P < 0.05$, **$P < 0.01$, ***$P < 0.001$). See Appendix Table S5 for additional repeats and statistical analysis for the survival data in this figure.
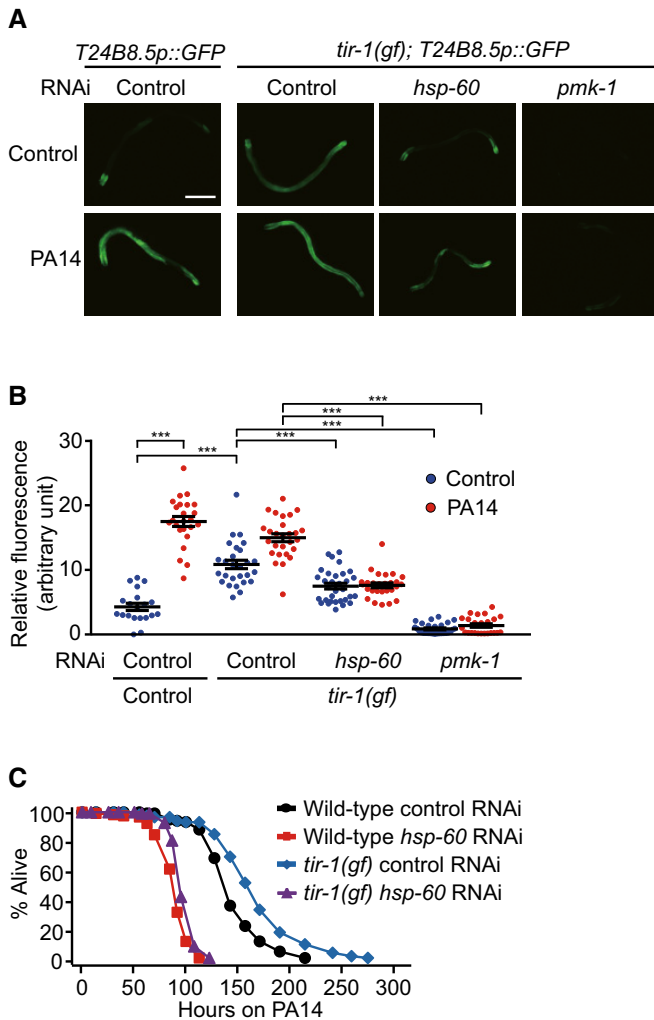
A

B

C

Figure 5. *hsp-60* is required for increased PA14 resistance and PMK-1 activity in *tir-1(gf)* animals.

A   Induction of *T24B8.5p::GFP* conferred by a *tir-1* gain-of-function (*gf*) mutation (*yz68*) was largely suppressed by knockdown of *hsp-60*. Scale bar indicates 200 μm.

B   Quantification of data in panel (A) (*n* ≥ 20). Error bars represent SEM. *P*-values were calculated by two-tailed Student's *t*-test (****P* < 0.001).

C   *hsp-60* RNAi largely suppressed the increased resistance of *tir-1(gf)* mutants to PA14.

Data information: See Appendix Table S6 for additional repeats and statistical analysis for the survival data in this figure.

PA14 resistance is not due to reduced fertility (Fig 6J). Together, these data suggest that enhanced survival on PA14 by increased expression of *hsp-60* is not due to overexpression artifacts or reduced fertility.

Increased expression of HSP-60/HSPD1 up-regulates PMK-1 signaling

We asked whether the PMK-1 signaling pathway mediated the effect of *hsp-60* on immunity. We found that *hsp-60::GFP* transgenes induced three PMK-1 downstream genes, in a *pmk-1*-dependent

manner (Fig 7A–C). *hsp-60::GFP* transgenes also increased the level of active phospho-PMK-1 (Fig 7D and Appendix Fig S5A). These data suggest that increased HSP-60 levels are sufficient for up-regulating PMK-1 signaling.

Mammalian HSPD1, the ortholog of *C. elegans* HSP-60, is also crucial for protein quality control in mitochondria. Therefore, we asked whether the regulation of p38 MAPK signaling by HSPD1 was conserved in mammals. Overexpression of human *HSPD1* accelerated the increase in the level of active phospho-p38 MAPK in cultured human cells at 2 h post-PA14 infection (HPI) (Fig 7E and Appendix Fig S5B). As p38 MAPK signaling plays key roles in mammalian immunity, this result raises a possibility that HSPD1/ HSP-60 exerts immune functions in mammals as well as in *C. elegans*.

HSP-60 increases PA14 resistance via stabilization of SEK-1/MKK3

We then examined the requirement of PMK-1 signaling components *pmk-1*, *sek-1/MKK3*, *nsy-1/ASK1*, and *tir-1/SARM* for the effect of *hsp-60::GFP* transgenes on susceptibility to PA14. We found that *pmk-1* or *sek-1* mutations largely suppressed the enhanced PA14 resistance conferred by *hsp-60::GFP* transgenes (Fig 7F and G), whereas *nsy-1* or *tir-1* mutations did not (Fig 7H and I). *sek-1* mutations also largely suppressed the induction of PMK-1-regulated genes conferred by *hsp-60::GFP* transgenes (Fig 7J–L). Thus, HSP-60 appears to act upstream of SEK-1 and PMK-1 to confer anti-PA14 resistance.

We further tested whether HSP-60 regulated the level or the localization of SEK-1 or PMK-1 proteins using tagRFP fusions expressed in the intestine. Importantly, we found that *hsp-60::GFP* transgenes increased the level of SEK-1::tagRFP, whereas transgenic expression of only GFP in the mitochondria (GFP^MT) did not (Fig 8A and B). We also showed that *hsp-60::GFP* transgenes did not affect the level of PMK-1::tagRFP (Fig 8C and D), or tagRFP in the intestine (Fig 8E and F). These data suggest that the increase in SEK-1:: tagRFP level by *hsp-60::GFP* transgenesis specific.

HSP-60 in the cytosol binds SEK-1/MKK3 and confers PA14 resistance

We then asked how mitochondrial HSP-60 increased the level of cytosolic SEK-1. A fraction of HSP-60 in yeast and cultured mammalian cells is known to be localized in the cytosol (Soltys & Gupta, 1996; Chun *et al*, 2010; Kalderon *et al*, 2015). Thus, we tested the possibility that a fraction of *C. elegans* HSP-60 in the cytosol up-regulated SEK-1. We first found that both endogenous and GFP-fused HSP-60 proteins were detected in the cytosol as well as in the mitochondria (Fig 9A and B). We then determined the functional importance of the HSP-60 in the cytosol, by expressing HSP-60::GFP lacking MTS, which was indeed localized in the cytosol (cytHSP-60:: GFP; Fig 9C–E). Importantly, we found that this *cythsp-60::GFP* enhanced PA14 resistance (Fig 9F).

Next, we asked whether the cytosolic HSP-60 physically interacted with SEK-1 by using a split GFP (spGFP) system (Ghosh *et al*, 2000; Hu *et al*, 2002; Zhang *et al*, 2004; Feinberg *et al*, 2008; Hiatt *et al*, 2008; Shyu *et al*, 2008). We detected green fluorescent signals in transgenic animals that expressed both N-terminal GFP fragment (spGFPN)-fused HSP-60 and C-terminal GFP fragment (spGFPC)-fused
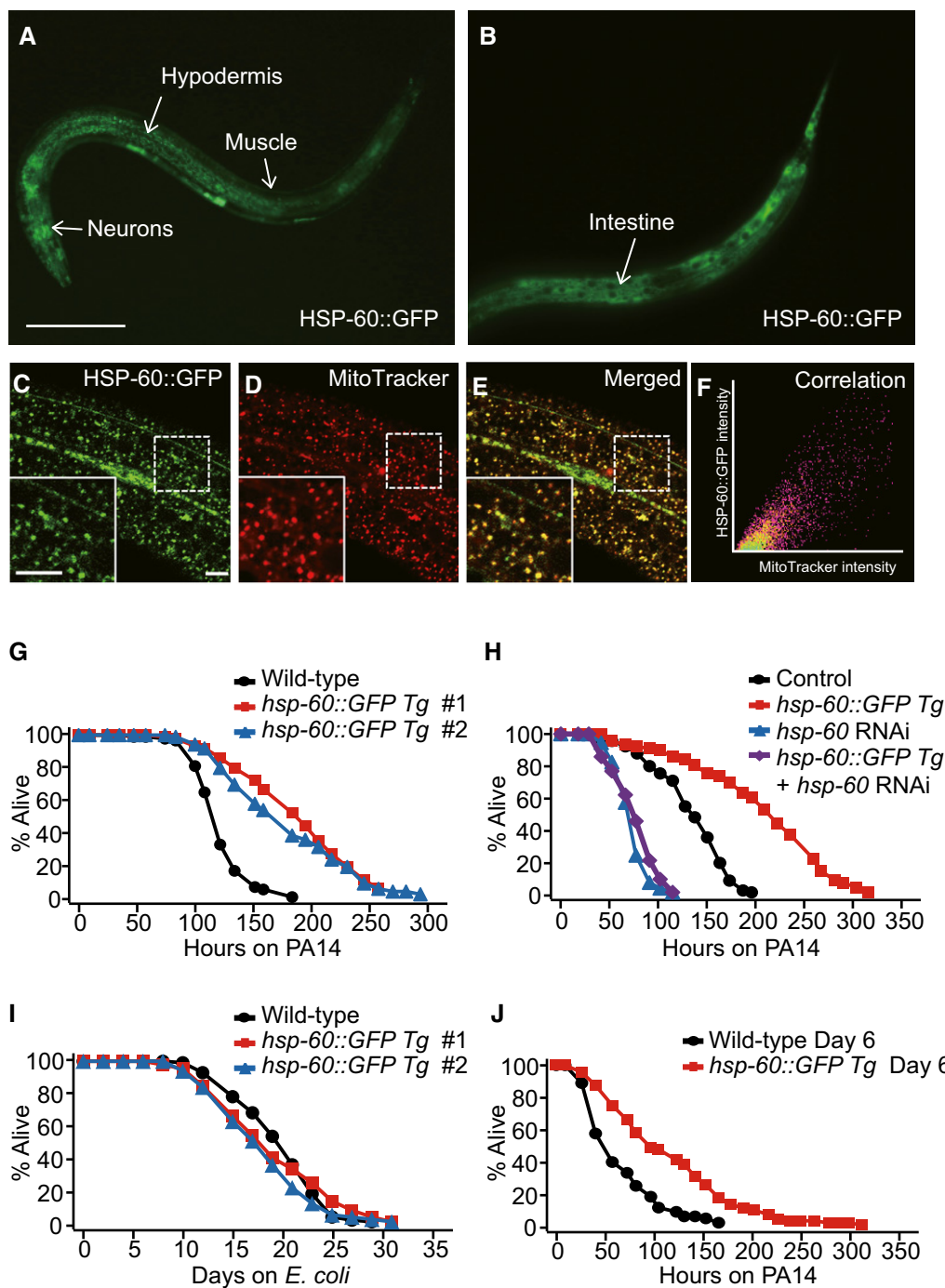
Figure 6. Increased expression of *hsp-60* is sufficient for increasing immunity against PA14.

A, B GFP fluorescence images of L4 larval animals that expressed *hsp-60::GFP*. GFP expression was observed in multiple tissues including neurons, the hypodermis, the muscles (A), and the intestine (B). Scale bar indicates 100 μm.

C–F Images of an L2 larval animal expressing HSP-60::GFP driven by an *hsp-60* promoter. HSP-60::GFP (C) and MitoTracker that stained mitochondria (D) were co-localized (E). Boxed areas were magnified in each panel. Scale bars indicate 10 μm. (F) HSP-60::GFP and MitoTracker signals (arbitrary units) in the boxed area in panel (E) showed significant correlation (Pearson's correlation coefficient: *r* = 0.917, *P* < 0.001). We also found that correlation between HSP-60::GFP and MitoTracker signals was significant by using the images of all 12 animals (Pearson's correlation coefficient: *r* = 0.906, *P* < 0.001).

G Two independent integrant lines of animals that expressed *hsp-60::GFP* (*hsp-60::GFP Tg*) were resistant to PA14.

H *hsp-60* RNAi abolished the increased survival of *hsp-60::GFP Tg* animals on PA14.

I *hsp-60::GFP Tg* animals lived slightly shorter on a normal *Escherichia coli* (OP50) diet.

J Day 6 post-reproductive *hsp-60::GFP Tg* animals displayed increased survival on PA14 without 5-fluoro-2′-deoxyuridine (FUdR) treatment.

Data information: See Appendix Tables S7 and S8 for additional repeats and statistical analysis for the survival and the lifespan data shown in this figure.
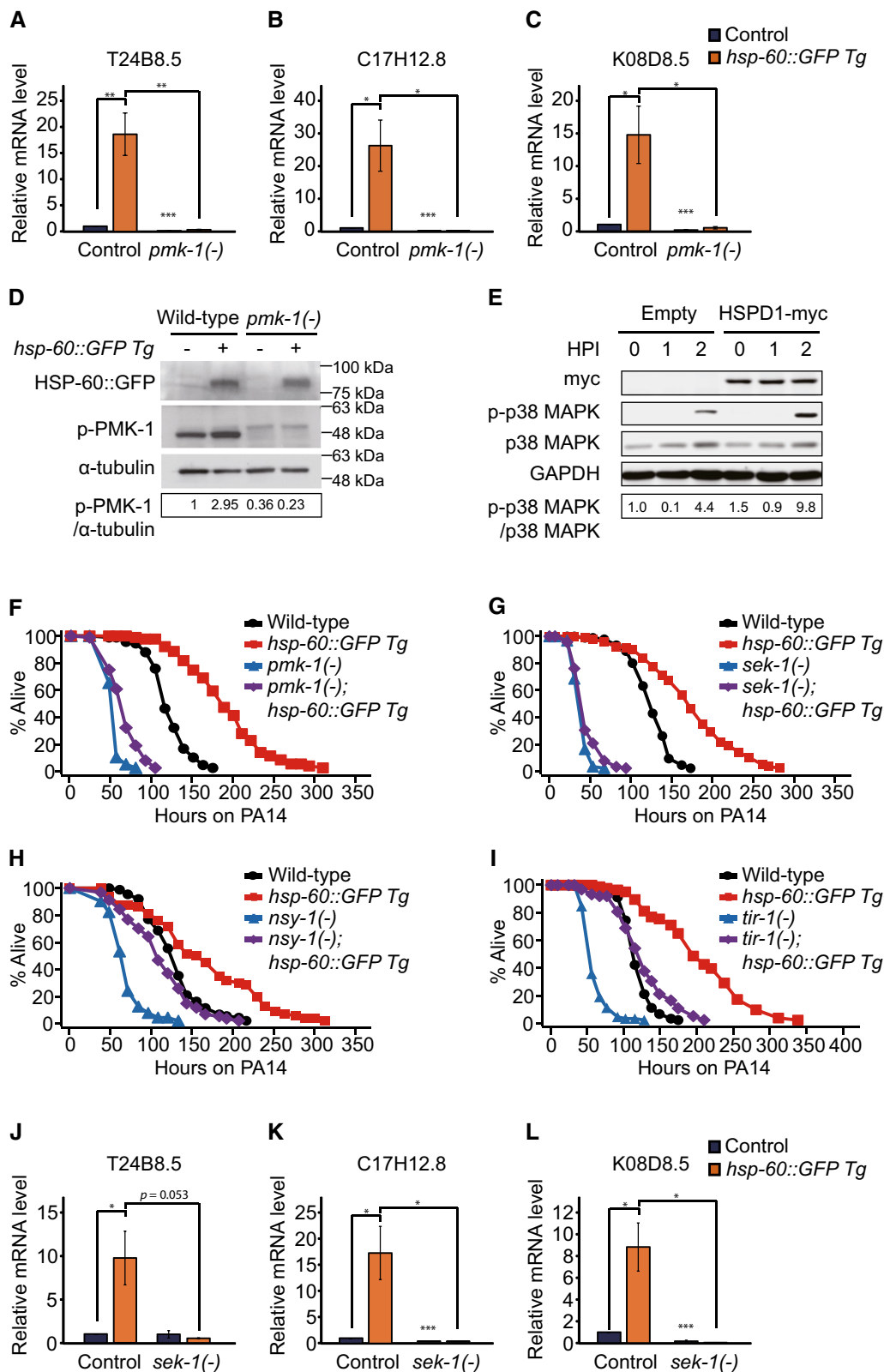
Figure 7.

SEK-1 (Fig 9G and H). This result indicates that HSP-60 binds SEK-1 (Fig EV4A). We used spGFPC fused with mitochondrial chaperone Y22D7AL.10, whose mammalian homolog HSPE1 interacts with

HSPD1/HSP60 in the mitochondria (Bukau & Horwich, 1998) and spGFPC, respectively, as positive and negative controls for HSP-60 binding (Figs EV4B–D, and 9J and K). We also noticed that the

Figure 7. HSP-60 up-regulates PMK-1 signaling and immunity against PA14 via SEK-1/MKK3.

A–C qRT–PCR analysis showed that three selected PMK-1 target genes, *T24B8.5* (A), *C17H12.8* (B) and *K08D8.5* (C), were induced by *hsp-60::GFP Tg* in a *pmk-1*-dependent manner without PA14 infection (*n* = 4).

D *hsp-60::GFP Tg* increased phospho-PMK-1 (p-PMK-1) level. α-tubulin was used as a loading control. GFP antibody was used for blotting HSP-60::GFP. The numbers below bands indicate relative intensities of the p-PMK-1 normalized to those of α-tubulin. The blot is a representative one out of four repeats that showed consistent results. See Appendix Fig S5A for quantification data.

E Western blot analyses were carried out by using HeLa cells expressing a myc-tagged human HSPD1 or a control plasmid (Empty: pcDNA3.1 pCMV-MYC). HSPD1-myc overexpression further increased the level of phospho-p38 MAP kinase (p-p38 MAPK), upon PA14 exposure for 2 h, but had little effect on the level of p38 MAP kinase (p38 MAPK). GAPDH was used as a loading control. HPI: hours post-infection. The numbers indicate relative intensities of the phospho-p38 MAPK level normalized to p38 MAPK level. The blot is a representative one of six repeats that showed consistent results. All six Western blot data are shown in the source data. See Appendix Fig S5B for quantification data.

F, G Enhanced PA14 resistance conferred by *hsp-60::GFP Tg* was largely suppressed by *pmk-1(km25)* mutation (F) or *sek-1(km4)* mutation (G).

H, I *hsp-60::GFP Tg* increased the survival of animals fed with PA14 in *nsy-1(ok593)* (H) and *tir-1(tm3036)* (I) mutants.

J–L qRT–PCR analysis showed that *sek-1* mutations largely suppressed the induction of three selected PMK-1 target genes, *T24B8.5* (J), *C17H12.8* (K) and *K08D8.5* (L), by *hsp-60::GFP Tg* without PA14 infection (*n* ≥ 3).

Data information: Error bars represent SEM. *P*-values were calculated by using two-tailed Student's *t*-test (*$P < 0.05$, **$P < 0.01$, ***$P < 0.001$). See Appendix Table S10 for additional repeats and statistical analysis for the survival data shown in this figure.

Source data are available online for this figure.

Discussion

In this report, we showed that the mitochondrial chaperone HSP-60 was necessary and sufficient for increasing immunity against *P. aeruginosa* by up-regulation of SEK-1/PMK-1 signaling. It is surprising that a single mitochondrial chaperone acted as the key effector and mediated immune signaling for the host defense. One possibility is that inhibition of mitochondrial chaperones impairs overall mitochondrial function, which in turn leads to reduced immunity against bacterial pathogens. However, this seems unlikely because genetic modulation that decreases mitochondrial function can actually increase anti-bacterial immunity (Hwang *et al*, 2014; Pellegrino *et al*, 2014). In addition, our data using *hsp-60::GFP* transgenic animals indicate that HSP-60 was sufficient to enhance immunity and immune-regulatory SEK-1/PMK-1 signaling. Thus, HSP-60 appears to increase SEK-1/PMK-1 pathway in the cytosol to modulate immunity against bacterial pathogens.

Our data suggest that HSP-60 located in the cytosol can play a role in immune responses. The effects of cytosolic HSP-60 on immunity led us to speculate that PA14 infection stress might trigger the translocation of HSP-60 from mitochondria to the cytosol. However, it does not seem to be the case, because PA14 infection did not alter the level of cytosolic HSP-60 or the ratio of cytosolic/mitochondrial HSP-60 levels (Figs 9A and B, and EV5A–C). In addition, cytosolic GFP signals obtained from the interaction between HSP-60::spGFPN and SEK-1::spGFPC were not increased by PA14 (Fig EV5D). These data suggest that a fraction of HSP-60 is localized in the cytosol under normal conditions and maintains SEK-1/PMK-1 signaling. A recent study using yeast showed that cytosolic HSP-60 inhibits 20S proteasome activity (Kalderon *et al*, 2015) in a chaperone function-independent manner. It will be interesting to test whether HSP-60 up-regulates SEK-1 through its

green fluorescence signals were located in the cytosol in the transgenic animals expressing spGFPN-fused HSP-60 and spGFPC-fused SEK-1 (Fig 9I). These results are consistent with the possibility that HSP-60 binds SEK-1 in the cytosol and stabilizes SEK-1. Altogether, our data suggest that HSP-60 in the cytosol binds and stabilizes SEK-1 to confer anti-bacterial defense in host animals.

chaperone function or through the inhibition of proteasome activity in *C. elegans*.

Intriguingly, a fraction of HSPD1/HSP60 in mammalian cells is shown to be localized in the extracellular space as well (Gupta & Knowlton, 2007; Cappello *et al*, 2008; Swaroop *et al*, 2016). Therefore, HSP-60 that is secreted to the extracellular space may also mediate immunity perhaps by acting as a cell-nonautonomous infection signal. We tested this possibility by measuring the tagRFP-fused HSP-60 signals in coelomocytes, which take up secreted proteins in *C. elegans* (Fares & Greenwald, 2001). We therefore expressed HSP-60::tagRFP specifically in the intestine or neurons, but did not detect the RFP signals in the coelomocytes (Appendix Fig S6A–D). Thus, we currently do not have data supporting the secretion of HSP-60 to extracellular space in *C. elegans*.

PA14 infection triggers mitochondrial stresses in *C. elegans*, and this in turn increases the level of HSP-60 at the transcription level through UPR^MT (Pellegrino *et al*, 2014). One interesting finding of our current study was that some components of UPR^MT, including DVE-1 and UBL-5, were required for the up-regulation of PMK-1, whereas other components, HAF-1 and ATFS-1, were not (Fig EV2E and F). This is actually consistent with the previous report showing that ATFS-1 enhances immunity against PA14 by the induction of anti-microbial genes independently of PMK-1 (Pellegrino *et al*, 2014). Thus, different UPR^MT components (e.g., ATFS-1 vs. HSP-60) appear to exert anti-bacterial functions via distinct immune signaling axes. In addition, Pellegrino *et al* (2014) concluded that activation of UPR^MT increases immunity independently of PMK-1, based on the results showing that RNAi targeting *spg-7* increases the survival of *pmk-1* mutants as well as wild-type animals on PA14. However, *spg-7* RNAi up-regulates many stress-responsive genes other than mitochondrial chaperones and increases lifespan (Curran and Ruvkun, 2007; Chen *et al*, 2007; Nargund *et al*, 2012). Thus, *spg-7* RNAi may increase the survival of *pmk-1* mutants through the activation of longevity and stress-responsive pathways independently of *pmk-1* signaling. Overall, UPR^MT appears to regulate at least two branches of anti-PA14 immune responses; one pathway acts through the induction of PMK-1-independent anti-microbial genes and the other pathway acts through the induction of mitochondrial chaperone genes, including *hsp-60* that increases immunity via *pmk-1* signaling.
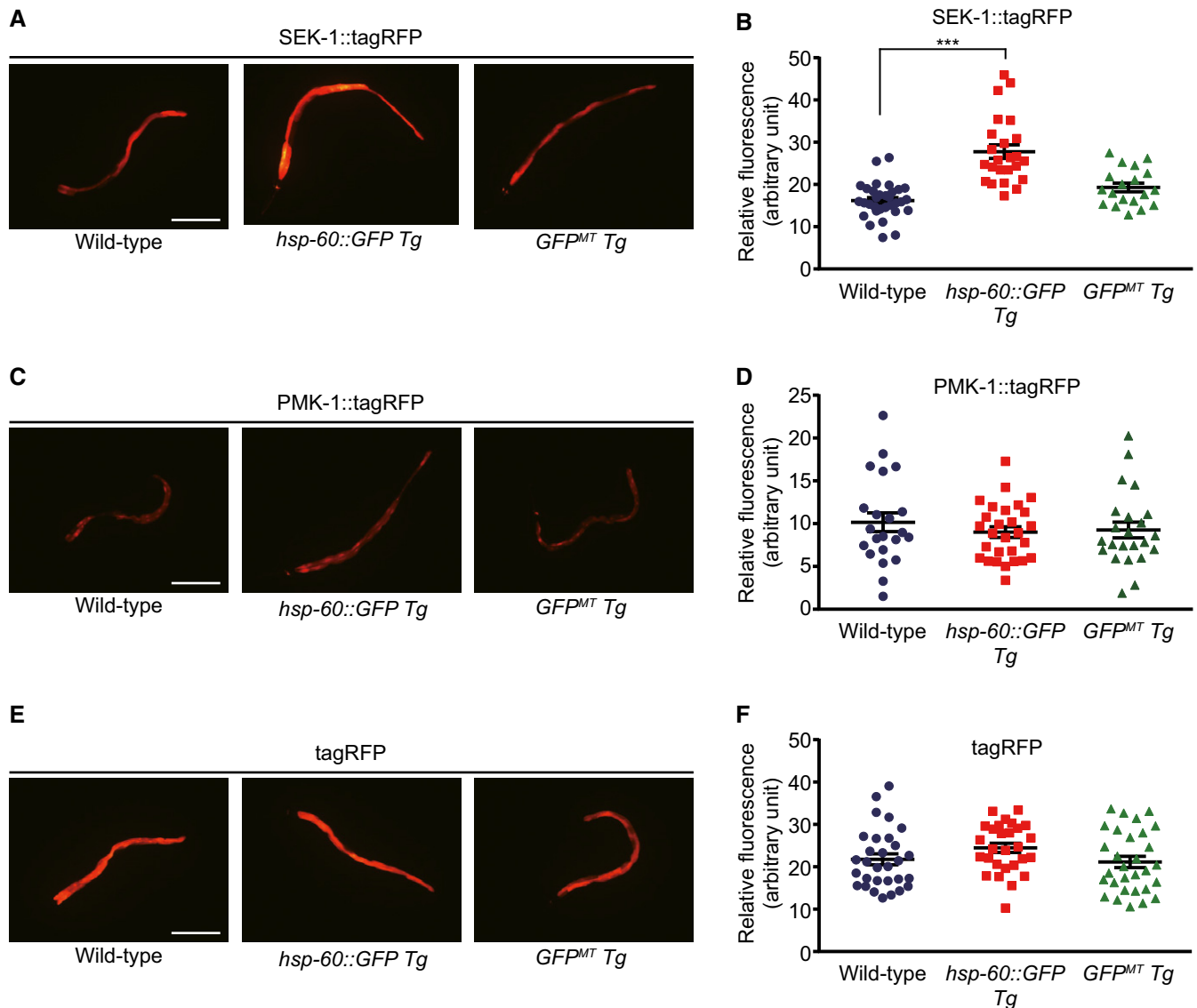
Figure 8. HSP-60 stabilizes SEK-1 in the cytosol of intestinal cells.

A, B   Representative images of young adult animals expressing SEK-1::tagRFP (A) driven by an intestine-specific *uha-6* promoter in wild-type, *hsp-60::GFP Tg* or *GFP^MT Tg* backgrounds. Quantification of data is shown in (B) ($n \geq 19$ from two independent trials).

C, D   Representative images of young adult animals expressing PMK-1::tagRFP (C) driven by an intestine-specific *uha-6* promoter in wild-type, *hsp-60::GFP Tg* or *GFP^MT Tg* backgrounds. Quantification of data is shown in (D) ($n \geq 22$ from two independent trials).

E, F   Representative images of young adult animals expressing tagRFP (E) driven by an intestine-specific *uha-6* promoter in wild-type, *hsp-60::GFP Tg* or *GFP^MT Tg* backgrounds. Quantification of data is shown in (F) ($n \geq 28$ from two independent trials).

Data information: Scale bars indicate 200 μm. Error bars represent SEM. Two-tailed Student's *t*-test was used for calculating *P*-values (***$P < 0.001$).

The potential regulatory role of HSPD1/HSP60 in p38 MAP kinase-dependent innate immune responses in mammals has been reported, but several key findings have been controversial. Treatment of immune cells such as macrophages and monocytes with recombinant human HSPD1/HSP60 (rhHSP60) purified from bacteria induces inflammatory cytokines (Chen *et al*, 1999), whose pro-inflammatory effects act through Toll-like receptor 4 (TLR4) and p38 MAP kinase signaling (Kol *et al*, 2000; Ohashi *et al*, 2000). However, several of these findings have been challenged by a report showing that the effects of the rhHSP60 were due to contamination with lipopolysaccharide (LPS) during protein purification processes from bacteria (Gao & Tsan, 2003). This finding has been supported by a subsequent study showing that a domain of HSPD1/HSP60 tightly binds to LPS (Habich *et al*, 2005). As LPS is a ligand for TLR4 and activates p38 MAP kinase signaling (O'Neill *et al*, 2013), the rhHSP60-dependent regulation of p38 MAP kinase signaling and immune functions remained controversial (Tsan & Gao, 2009; Quintana & Cohen, 2011). Our current study provides crucial *in vivo* evidence for addressing this issue. First, our data with *hsp-60* RNAi indicate that endogenous HSPD1/HSP60 is required for the
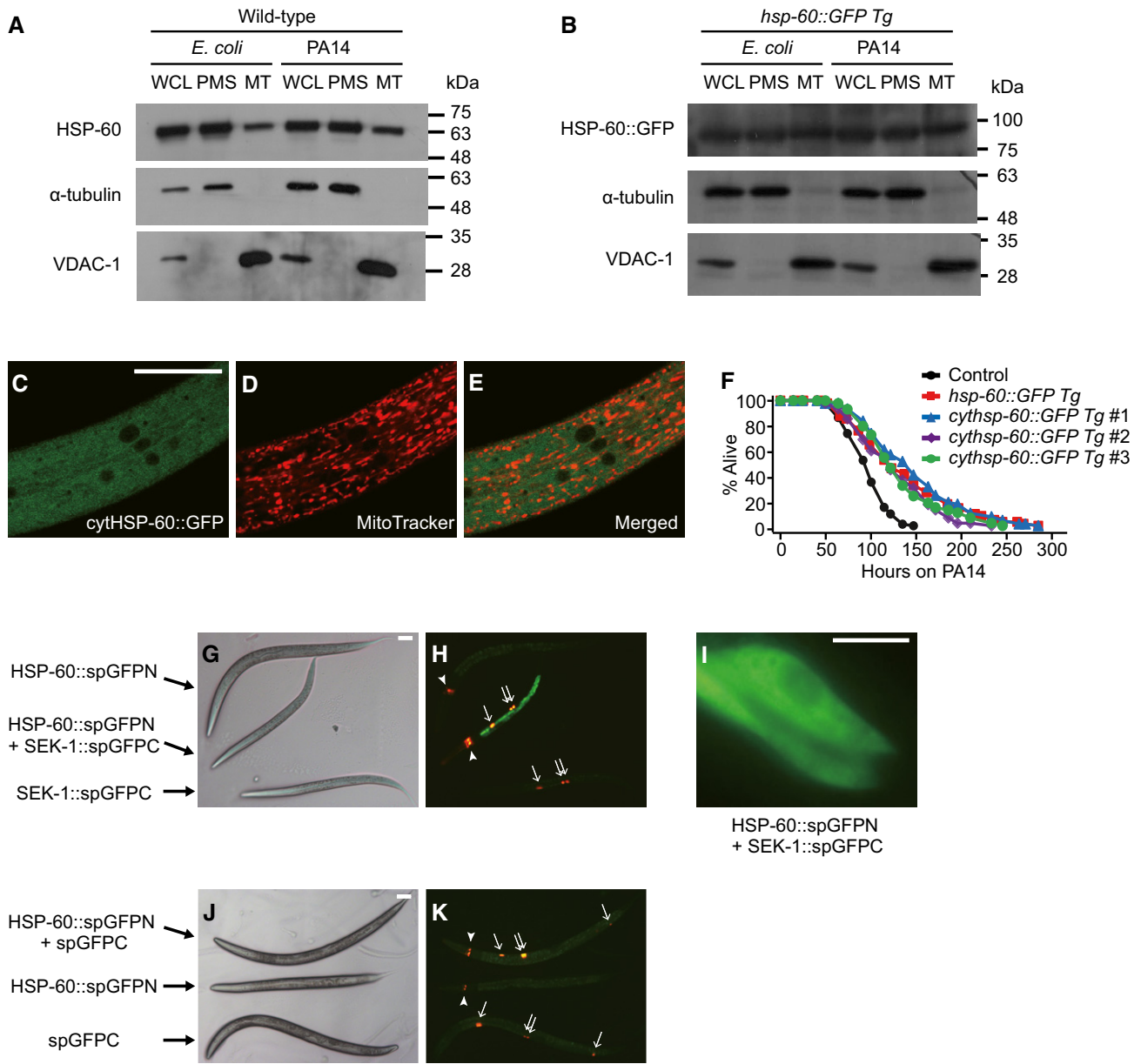
Figure 9. A fraction of HSP-60 is localized in the cytosol and physically interacts with SEK-1.

A, B Western blot analyses showed that endogenous HSP-60 (A) and GFP-fused HSP-60 (B) were detected in both mitochondrial (MT) and post-mitochondrial supernatant (PMS) fractions upon infection with PA14 for 12 h. WCL indicates whole-cell lysate. α-tubulin and VDAC-1 were used as markers of PMS and mitochondria, respectively. The blots in these two panels are representative ones out of five (A) and three repeats (B), respectively. Note that the levels of HSP-60 in the PMS were reproducibly higher than those in MT, but the majority of GFP-fused HSP-60 signals are localized to mitochondria (Fig 6C–F). It seems likely that the volume of the mitochondria is smaller than that of the non-mitochondrial parts, and this may underlie the strong GFP-fused HSP-60 signals in the mitochondria.

C–E Images of an L2 larval animal expressing HSP-60::GFP lacking mitochondrial targeting sequence at the N-terminus (cytHSP-60::GFP) driven by an *hsp-60* promoter. cytHSP-60::GFP (C) was not co-localized with mitochondria stained by using MitoTracker (D) as shown in the merged image (E). Scale bar indicates 25 μm.

F Three independent lines of transgenic animals that expressed *cythsp-60::GFP* (*cythsp-60::GFP Tg*) were resistant to PA14 infection. The transgenic animals that expressed *hsp-60::GFP* with intact mitochondrial targeting sequence (*hsp-60::GFP Tg*) were used as a positive control.

G–I Bright field (G) and fluorescence (H) images of the animals that expressed an N-terminal GFP fragment fused with HSP-60 (HSP-60::spGFPN) and/or a C-terminal GFP fragment fused with SEK-1 (SEK-1::spGFPC) driven by an intestine-specific *uha-6* promoter. Among siblings from the same hermaphrodite, transgenic animals that expressed both HSP-60::spGFPN and SEK-1::spGFPC displayed the GFP signals in the cytosol (I) (*n* = 10). Arrowheads indicate *odr-1p::RFP*, a co-injection marker for HSP-60::spGFPN. Arrows indicate *coel::RFP*, a co-injection marker for SEK-1::spGFPC. Scale bars indicate 50 μm.

J, K Representative bright field (J) and fluorescence (K) images of the animals that expressed HSP-60::spGFPN and/or C-terminal GFP fragment (spGFPC) driven by the intestine-specific *uha-6* promoter. None of these transgenic animals displayed green fluorescence signals. Arrowheads indicate *odr-1p::RFP*, a co-injection marker for HSP-60::spGFPN. Arrows indicate *coel::RFP*, a co-injection marker for spGFPC. Scale bars indicate 50 μm.

Data information: See Appendix Table S11 for additional repeats and statistical analysis for the survival data shown in this figure. See Fig EV4B–D for the positive control experiment for the spGFP system.

maintenance of p38 MAP kinase signaling. Second, we showed that genetic up-regulation of HSP60/HSPD1, which is free from LPS contamination, increased p38 MAP kinase signaling both in *C. elegans,* and cultured mammalian cells. Thus, our study strongly supports the notion that HSPD1/HSP60 enhances immunity.

Mammalian HSPD1/HSP60 elicits immune responses via immune regulators other than p38 MAP kinase signaling as well. The induction of mitochondrial HSPD1/HSP60 is implicated in TNF-α-mediated activation of NF-κB, a key immunity transcription factor in mammalian cells (Amberger *et al*, 1997; Chun *et al*, 2010). HSPD1/HSP60 activates interferon-regulatory factor 3 (IRF3) and increases interferon production in cultured cells (Lin *et al*, 2014). Overall, these studies and our current work suggest that both *C. elegans* and mammals share common mechanisms that employ the mitochondrial chaperone HSP-60/HSPD1 to boost immunity.

Materials and Methods

Caenorhabditis elegans strains

All strains were maintained as previously described (Stiernagle, 2006). Some strains were obtained from Caenorhabditis Genetics Center, which is funded by the NIH National Center for Resources (P40 OD010440). Strains analyzed in this study were listed as follows: N2 wild-type, IJ130 *pmk-1(km25) IV* obtained by outcrossing KU25 four times to Lee laboratory N2, IJ134 *zip-2(tm4067) III* obtained by outcrossing TM4067 four times to Lee laboratory N2, IJ382 *daf-16 (mu86) I* obtained by outcrossing CF1042 six times to Kenyon laboratory N2, which is the same as Lee laboratory N2, AU78 *agIs219 [T24B8.5p::GFP]* a gift from D.H. Kim laboratory, AU133 *agIs17[irg-1p::GFP]* a gift from E. Troemel laboratory, CL2166 *dvIs19[gst-4p:: GFP::NLS]*, CF1553 *muIs84[sod-3p::gfp]*, WM27 *rde-1(ne219) V*, VP303 *rde-1(ne219) V; kzIs7[nhx-2p::rde-1; rol-6(su1006)]*, NR350 *rde-1(ne219) V; kzIs20[hlh-1p::rde-1; sur-5p::NLS::GFP]*, NR222 *rde-1 (ne219) V; kzIs9[lin-26p::rde-1; lin-26p::nls::GFP; rol-6(su1006)]*, NL3321 *sid-1(pk3321) V*, TU3401 *sid-1(pk3321) V; uIs69[myo-2p:: mCherry; unc-119p::sid-1]*, IJ574 *haf-1(ok705) V* obtained from outcrossing RB867 four times to Lee laboratory N2, IJ575 *atfs-1 (gk3094) V* obtained from outcrossing VC3201 four times to Lee laboratory N2, IJ283 *tir-1(yz68) III* obtained from outcrossing *tir-1 (yz68)*, a gift from J.Y. Sze laboratory, four times to Lee laboratory N2, IJ698 *haf-1(ok705) V; agIs219[T24B8.5p::GFP; ttx-3p::GFP]*, IJ702 *atfs-1(gk3094) V; agIs219[T24B8.5p::GFP; ttx-3p::GFP]*, IJ819 *tir-1 (yz68) III; agIs219[T24B8.5p::GFP; ttx-3p::GFP]*, AY101 *acIs101 [F35E12.5p::GFP; rol-6(su1006)]*, IJ530 *yhEx121[odr-1p::RFP]*, IJ788 *yhEx188[hsp-60p::hsp-60::GFP; odr-1p::RFP]* marked as #3 in Fig EV3E and G, IJ789 *yhEx189[hsp-60p::hsp-60::GFP; odr-1p::RFP]* marked as #4 in Fig EV3E, IJ790 *yhEx190[hsp-60p::hsp-60::GFP; odr-1p::RFP]* marked as #5 in Fig EV3E, IJ939 *yhIs62[hsp-60p::hsp-60::GFP; odr-1p::RFP]* marked as #1 in Figs 6G–I and EV3A–C, obtained from integration of *yhEx188* and subsequent outcrossing four times to Lee laboratory N2, IJ940 *yhIs63[hsp-60p::hsp-60::GFP; odr-1p::RFP]* marked as #2 in Figs 6G–I and EV3A–C, obtained from integration of *yhEx188* and subsequent outcrossing four times to Lee laboratory N2, IJ1141 *yhEx253[hsp-60p::GFP^{MT}; odr-1p::RFP]* marked as GFP^{MT} Tg #1 in Appendix Fig S3D, IJ1142 *yhEx254[hsp-60p::GFP^{MT}; odr-1p::RFP]* marked as GFP^{MT} Tg #2 in Appendix Fig S3D, IJ1143 *yhEx255*

[hsp-60p::GFP^{MT}; odr-1p::RFP] marked as GFP^{MT} Tg #3 in Appendix Fig S3D, IJ941 *pmk-1(km25) IV; yhIs62[hsp-60p::hsp-60::GFP; odr-1p:: RFP]*, IJ1324 *sek-1(km4) X; yhIs62[hsp-60p::hsp-60::GFP; odr-1p:: RFP]*, IJ1325 *nsy-1(ok593) II; yhIs62[hsp-60p::hsp-60::GFP; odr-1p:: RFP]*, IJ942 *tir-1(tm3036) III; yhIs62[hsp-60p::hsp-60::GFP; odr-1p:: RFP]*, IJ1307 *yhEx332[vha-6p::tagRFP; ofm-1p::GFP]*, IJ1310 *yhEx335 [vha-6p::pmk-1::tagRFP; ofm-1p::GFP]*, IJ1313 *yhEx338[vha-6p::sek-1::tagRFP; ofm-1p::GFP]*, IJ1360 *yhIs62[hsp-60p::hsp-60::GFP; odr-1p::RFP]; yhEx332[vha-6p::tagRFP; ofm-1p::GFP]*, IJ1361 *yhIs62 [hsp-60p::hsp-60::GFP; odr-1p::RFP]; yhEx335[vha-6p::pmk-1:: tagRFP; ofm-1p::GFP]*, IJ1362 *yhIs62[hsp-60p::hsp-60::GFP; odr-1p:: RFP]; yhEx338[vha-6p::sek-1::tagRFP; ofm-1p::GFP]*, IJ1363 *yhEx253 [hsp-60p::GFP^{MT}; odr-1p::RFP]; yhEx332[vha-6p::tagRFP; ofm-1p:: GFP]*, IJ1364 *yhEx253[hsp-60p::GFP^{MT}; odr-1p::RFP]; yhEx335[vha-6p::pmk-1::tagRFP; ofm-1p::GFP]*, IJ1365 *yhEx253[hsp-60p::GFP^{MT}; odr-1p::RFP]; yhEx338[vha-6p::sek-1::tagRFP; ofm-1p::GFP]*, IJ650 *yhEx153[fasn-1p::GFP; odr-1p::RFP]*, IJ1464 *yhEx399[hsp-60p::hsp-60; fasn-1p::GFP]* marked as *hsp-60 Tg #1* in Fig EV3D and F, IJ1464 *yhEx399[hsp-60p::hsp-60; fasn-1p::GFP]* marked as *hsp-60 Tg #2* in Fig EV3D and F, IJ1169 *yhEx260[hsp-60p::cythsp-60::GFP; odr-1p:: RFP]* marked as *cythsp-60::GFP Tg #1* in Fig 9F, IJ1170 *yhEx261[hsp-60p::cythsp-60::GFP; odr-1p::RFP]* marked as *cythsp-60::GFP Tg #2* in Fig 9F, IJ1171 *yhEx262[hsp-60p::cythsp-60::GFP; odr-1p::RFP]* marked as *cythsp-60::GFP Tg #3* in Fig 9F, IJ1420 *yhEx381[vha-6p:: hsp-60::tagRFP; odr-1p::RFP]*, IJ1423 *yhEx384[unc-119p::hsp-60:: tagRFP; fasn-1p::GFP]*, IJ1436 *yhEx389[vha-6p::hsp-60::spGFPN; odr-1p::RFP]; yhEx391[vha-6p::sek-1::spGFPC; coel::RFP]*, IJ1438 *yhEx389 [vha-6p::hsp-60::spGFPN; odr-1p::RFP]; yhEx395[vha-6p::spGFPC; coel::RFP]*, IJ1441 *yhEx389[vha-6p::hsp-60::spGFPN; odr-1p::RFP]; yhEx397[vha-6p:: Y22D7AL.10::spGFPC; coel::RFP]*.

Selection of evolutionarily conserved mitochondrial genes

By using the HomoloGene (build 25) database of NCBI (National Center for Biotechnology Information), a total of 3,147 *C. elegans* genes that have single orthologous human genes were selected (WormBase web site, http://www.wormbase.org, WS229, released on December 15th, 2011). When more than two *C. elegans* genes were matched to a single human gene, these genes were excluded from further study to avoid potential limitations in data interpretation due to genetic redundancy. Subsequently, 313 mitochondrial genes were selected for the ones that were annotated with mitochondria in human MitoCarta database (Pagliarini *et al*, 2008) (https://www.broadinstitute.org/pubs/MitoCarta/human.mitocarta.html) and with mitochondrial Gene Ontology terms (Ashburner *et al*, 2000; Gene Ontology Consortium, 2015); 0000266 (mitochondrial fission), 0005739 (mitochondrion), 0005740 (mitochondrial envelope), 0005741 (mitochondrial outer membrane), 0005743 (mitochondrial inner membrane), 0005759 (mitochondrial matrix), 0008053 (mitochondrial fusion), 0030061 (mitochondrial crista), 0031966 (mitochondrial membrane), and 0044429 (mitochondrial part) from "gene_info" file and "gene2go" file of NCBI FTP database.

RNAi screen

RNAi clones targeting 244 genes of the 313 mitochondrial genes that we selected were available in two commercial *C. elegans* RNAi feeding libraries generated by Ahringer laboratory (Geneservice Ltd.,

Cambridge, UK) or by Vidal laboratory (Source BioScience, Nottingham, UK). We initially tested these 244 RNAi clones for developmental phenotypes and selected 220 RNAi clones that did not cause severe developmental delay or lethality for further studies (see Dataset EV1). RNAi bacteria were cultured overnight at 37°C in Luria Broth (LB) media containing 50 μg/ml ampicillin (USB, Santa Clara, CA, USA), seeded onto nematode-growth media (NGM) containing 50 μg/ml ampicillin, and then incubated overnight at 37°C. The bacteria were treated with 1 mM isopropyl β-D-1-thiogalactopyranoside (IPTG: GOLDBIO, St. Louis, MO, USA) overnight at 37°C for the induction of double-stranded RNA (dsRNA). Wild-type N2 worms were then fed with the RNAi bacteria and grown to L4 or young adult stages. Approximately 100 worms at L4 or young adult stage were subjected to PA14 standard slow killing assays at 25°C (see pathogen killing assays described below for detail). Worms that were moving were counted as alive every 12–24 h until all the worms were dead. From our initial screen, we chose 46 out of the 220 RNAi clones that substantially altered the susceptibility of animals to PA14 infection (arbitrary cutoff: % change in mean survival vs. control group > ±10%, *P*-value < 0.001). Subsequent experiments confirmed that 16 RNAi clones reproducibly increased or decreased the survival of wild-type animals on PA14. OASIS (Online Application of Survival analysIS, http://sbi.postech.ac.kr/oasis) was used for statistical analysis of survival data, and *P*-values were calculated by using log-rank (Mantel–Cox method) test (Yang *et al*, 2011).

Characterization and clustering analysis of candidate genes

Changes in mean survival and GFP reporter levels for known immune effectors were measured for the initial analysis of the 16 RNAi clones obtained from our screen. First, upon knocking down each of the 16 RNAi clones, two independent trials of PA14 standard slow killing assays were performed by using worms in different genetic backgrounds; *pmk-1(km25)*, *zip-2(tm4067)*, and *daf-16 (mu86)*. OASIS (http://sbi.postech.ac.kr/oasis) was used for statistical analysis of survival data, which uses log-rank (Mantel–Cox method) test for calculating *P*-values (Yang *et al*, 2011). Second, GFP reporter transgenic animals for known immune effector proteins (*T24B8.5p::GFP* for PMK-1, *irg-1p::GFP* for ZIP-2, *gst-4p::GFP* for SKN-1, and *sod-3p::GFP* for DAF-16) were fed with the RNAi bacteria from egg to L4 or young adult stages and subsequently transferred to the corresponding dsRNA-expressing *E. coli*- or PA14-seeded plates. After 24 h, the effects of each of the 16 RNAi clones on the expression of the GFP reporters were scored by three researchers at least three times independently. By using Cluster 3.0 (de Hoon *et al*, 2004), the genes were hierarchically clustered (clustering method: complete linkage, similarity matrix: City Block) based on the effects of RNAi clones on the survival of animals on PA14 and the GFP reporter expression as shown in the heat maps (Fig 1C and D).

Pathogen killing assays

PA14 standard slow killing assay was performed as previously described (Reddy *et al*, 2009) with minor modifications. PA14 was cultured in LB media at 37°C overnight, and 5 μl of the culture was seeded onto the center of the NGM plates containing 0.35%

peptone. PA14-seeded plates were then incubated at 37°C for 24 h and stored at room temperature for at least 8 h before use. Worms were grown from egg to L4/young adult stages on RNAi bacteria- or OP50-seeded plates at 20°C. The worms were then transferred to PA14-seeded plates containing 50 μM 5-fluoro-2′-deoxyuridine (FUdR; Sigma, St Louis, MO, USA, or bioWORLD, Dublin, OH, USA), which prevents progeny from hatching, at 25°C. The worms were scored twice or three times a day and counted as dead if the worms did not respond to prodding. For PA14 killing assays without FUdR, the animals were transferred twice a day to fresh PA14-seeded plates for removing the progeny. Animals that showed internal hatching were counted as dead, while those that crawled off the plates, exploded or burrowed were censored but included in the subsequent statistical analysis. OASIS (http://sbi.postech.ac.kr/oasis) was used for statistical analysis of survival data, and *P*-values were calculated by using log-rank (Mantel–Cox method) test (Yang *et al*, 2011). Pathogen resistance assays against *E. faecalis* or pathogenic *E. coli* were performed as previously described (Garsin *et al*, 2001; Hwang *et al*, 2014).

Microscopy

Transgenic animals that expressed *GFP* or *tagRFP* were anesthetized by using 100 mM sodium azide (DAEJUNG, Siheung, Korea) and subsequently imaged by using AxioCam HRc (Zeiss Corporation, Jena, Germany) camera mounted on a Zeiss Axioscope A.1 microscope (Zeiss Corporation, Jena, Germany). The fluorescence intensity of the animals was quantified by using ImageJ software (Rasband, W.S., ImageJ, U. S. National Institutes of Health, Bethesda, MD, USA, http://rsb.info.nih.gov/ij/) and displayed by using GraphPad Prism 7 software (http://www.graphpad.com/scientific-software/prism/). Mitochondrial staining with MitoTracker Red CMXRos (catalogue number: M7512, Life Technologies™, Eugene, OR, USA) was conducted as described previously (Govindan *et al*, 2015) with minor modifications. The MitoTracker was added to OP50-seeded NGM plates at a final concentration of 10 μM. After the plates were dried, *hsp-60p::hsp-60::GFP*, *hsp-60p::GFP^MT*, and *hsp-60p::cythsp-60::GFP* worms were transferred to the plates. Six hours after this initial transfer, the animals were transferred again to fresh OP50-seeded NGM plates to remove the MitoTracker from the intestinal lumen for 1–2 h. The animals were subsequently transferred onto a 2% agarose pad and were photographed by using the Nikon A1si/Ni-E upright confocal microscope with 60×, 1.4 NA oil-immersion objective lens. Confocal microscopy data were acquired at the Advanced Neural Imaging Center in Korea Brain Research Institute (KBRI). To measure developmental rates, synchronized wild-type eggs were grown on control, *spg-7*, or *cco-1* RNAi bacterial plates or EtBr (30 μg/ml)-treated control RNAi bacterial plates for 3 days. The eggs of *hsp-60p::hsp-60::GFP* worms were grown on control RNAi plates for 3 days. The images of the animals on the plates were captured by using a DIMIS-M camera (Siwon Optical Technology, Anyang, Korea).

Intestinal PA14-GFP accumulation assays

Intestinal PA14-GFP accumulation assays were performed as previously described (Kim *et al*, 2002) with minor modification. To measure the amount of accumulated PA14 in the *C. elegans*

intestine, L4 worms that were pre-treated with control RNAi or *hsp-60* RNAi were infected with PA14 that expressed GFP (PA14-GFP) for 48 h. Five microliters of overnight culture of PA14-GFP in LB media containing 50 μg/ml kanamycin (Sigma, St Louis, MO, USA) was seeded onto the center of NGM plates that contained 0.35% peptone and 50 μM FUdR. Plates were incubated at 37°C for 24 h and then stored at room temperature at least for 8 h before use. *P*-values were calculated by using chi-squared test.

PA14 avoidance assays

PA14 avoidance assays were performed as previously described (Pradel *et al*, 2007; Gaglia *et al*, 2012) with some modifications. Wild-type animals were allowed to develop on control or *hsp-60* RNAi bacteria from egg to L4 stages. Five microliters of overnight PA14 culture was seeded onto the center of 0.35% peptone NGM. Plates were incubated at 37°C for 24 h and subsequently at room temperature for over 8 h before use. At least 20 L4 stage worms were transferred to a control *E. coli-* or a PA14-seeded plate, and the number of occupants on the bacterial lawn was counted at indicated time points.

Lifespan analyses

Lifespan analyses were performed as previously described (Lee *et al*, 2015). Briefly, synchronized wild-type eggs were allowed to develop on control and *hsp-60* RNAi plates to young adult stage and then transferred to 5 μM FUdR-containing control and *hsp-60* RNAi plates, respectively. The number of worms that were alive was counted at 2 or 3 day intervals. Control animals or transgenic animals that expressed *hsp-60p::hsp-60::GFP* were grown on OP50 plates and subjected to lifespan assays. *odr-1p::RFP* (an injection marker) animals were used as a control for transgenic animals that expressed extrachromosomal arrays of *hsp-60p::hsp-60::GFP* or *hsp-60p::GFP^MT*. Wild-type (N2) animals were used as a control for integrated lines of *hsp-60p::hsp-60::GFP* animals, as integrated lines of *odr-1p::RFP* were not available. The animals that crawled off the plates, displayed ruptured vulvae, burrowed, or displayed internal hatching were censored but included in the subsequent statistical analysis. Statistical analysis of lifespan data was performed by using OASIS (http://sbi.postech.ac.kr/oasis), which calculates *P*-values using log-rank (Mantel–Cox method) test (Yang *et al*, 2011).

Western blot assays

Western blot assays were conducted as described previously (Hwang *et al*, 2014) with minor modifications. Synchronized eggs were placed on control RNAi, *hsp-60* RNAi, or *pmk-1* RNAi bacteria-seeded NGM plates containing 50 μg/ml ampicillin and 1 mM IPTG. Worms were then allowed to develop to L4 or young adult animals. Mixed L4 and young adult animals were washed three times by using M9 buffer and subsequently transferred onto corresponding RNAi bacteria- or PA14-seeded plates (0.35% peptone NGM plates). After 1 h of PA14 exposure, the worms were washed at least three times with M9 and immediately frozen in liquid nitrogen with 2× SDS sample buffer. The samples were subsequently boiled for 10 min at 95°C and vortexed for 10 min at room temperature for protein extraction. The lysates were further centrifuged for 30 min

at 15,700 *g*, and supernatants without debris were used for 8% SDS–PAGE. After electrophoresis, proteins were transferred to PVDF membrane (Whatman Inc, Sanford, ME, USA). Five percent BSA or skim milk in TBS-T [20 mM Tris–HCl (pH 7.6), 140 mM NaCl, 0.1% Tween-20] was used for blocking the PVDF membrane for an hour. The PVDF membrane was then incubated with primary antibodies against α-tubulin (1:1,000, Santa Cruz Biotechnology, sc-32293, Dallas, TX, USA), phospho-p38 MAPK (1:1,000, Cell Signaling, #9211, Beverly, MA, USA), HSP-60 (1:100,000, Enzo Life Sciences, ADI-SPA-807, Farmingdale, NY, USA) or GFP (1:5,000, in-house rabbit polyclonal antibody). Anti-mouse secondary antibody conjugated with horseradish peroxidase (1:5,000, Thermo, Rockford, IL, USA) was used for detecting anti-α-tubulin, and anti-rabbit secondary antibody (1:7,500, Thermo, Rockford, IL, USA) was used for detecting anti-phospho-p38 MAPK and anti-GFP primary antibodies. The PVDF membrane was treated with chemoluminescent horseradish peroxidase substrate (Thermo, Rockford, IL, USA) for detecting protein bands. For Western blot analysis using transgenic animals overexpressing *hsp-60::GFP*, synchronized eggs of wild-type animals, *pmk-1* mutant animals, and the *hsp-60::GFP* transgenic animals were allowed to develop to young adults on OP50 plates and then were harvested as described above after washing three times with M9 buffer. For Western blot assays using a cultured cell line, HeLa cells were maintained in DMEM (LonZa, Walkersville, MD, USA) supplemented with 10% fetal bovine serum (HyClone™, GE Healthcare Life Sciences, South Logan, UT, USA) and transfected with pCMV-MYC or pCMV-HSPD1-MYC by using Effectene (Qiagen, Valencia, CA, USA) following the manufacturer's protocol. Primary antibodies against GAPDH (Merck Millipore, Darmstadt, Germany) and α-tubulin (Santa Cruz, CA, USA) were used for the detection of GAPDH and α-tubulin, respectively. MYC antibody (Santa Cruz, CA, USA) was used for the detection of MYC-tagged HSPD1.

Fractionation of mitochondria

Mitochondrial fractionation was performed as previously described (Jonassen *et al*, 2002) with minor modifications. Experimental samples for synchronized wild-type or *hsp-60p::hsp-60::GFP* animals under *E. coli-* or PA14-fed conditions were prepared as described above. The animals were harvested after washing at least three times with M9 buffer. The worm samples were transferred to pre-cooled mitochondria isolation buffer [MIB; 210 mM mannitol, 70 mM sucrose, 0.1 mM EDTA, 5 mM Tris–HCl (pH 7.4), 1 mM PMSF] and then subjected to homogenization. The samples were homogenized by using pre-cooled glass homogenizer with 20 strokes. The supernatants were transferred to new microtubes, and remaining worm pellets were resuspended with the MIB and homogenized. The supernatants were collected by centrifugation for 10 min at 800 relative centrifugal force (rcf), transferred to new microtubes and kept as whole-cell lysates (WCL). The WCL were further centrifuged for 10 min at 22,250 *g*, and the supernatants were collected without touching the pellets and stored as post-mitochondrial supernatants (PMS). Remaining pellets were resuspended with MIB and then centrifuged again at 22,250 *g* for 10 min. The supernatants were discarded, and remaining pellets were resuspended with MIB and stored as mitochondrial fraction (MT). Western blot analyses with WCL, PMS, and MT proteins were performed as described above. Primary antibodies against α-tubulin (1:1,000, Santa Cruz Biotechnology, Dallas, TX,

USA), VDAC-1 (1:1,000, Santa Cruz Biotechnology, sc-8828, Dallas, TX, USA), HSP-60 (1:100,000, ADI-SPA-807, Enzo Life Sciences, Farmingdale, NY, USA), or GFP (1:5,000, in-house rabbit polyclonal antibody) were used for the Western blot analyses.

RNA extraction and quantitative real-time PCR

RNA extraction and qRT–PCR were performed as previously described with minor modifications (Seo *et al*, 2015). Worms fed with control RNAi, *pmk-1* RNAi, or *hsp-60* RNAi bacteria were grown to L4 stage and then transferred to PA14-seeded plates after washing with M9 buffer 3–4 times. Wild-type, *pmk-1(−)*, and *sek-1(−)* animals or transgenic animals expressing *hsp-60p::hsp-60::GFP* were allowed to develop on OP50-seeded plates to young (day 1) adults. Worms were harvested by washing three or four times with M9 buffer to remove residual bacteria 8 h after PA14 exposure. Total RNA in the animals was isolated by using RNAiso plus (Takara, Seta, Kyoto, Japan) and was used for synthesizing cDNA with ImProm-II™ Reverse Transcriptase kit (Promega, Madison, WI, USA). Quantitative real-time PCR was performed by using StepOne Real-Time PCR System (Applied Biosystems, Foster City, CA, USA) as described in the manufacturer's protocol. Comparative C_T method was used for the quantitative analysis of mRNAs. For all biological data sets, *ama-1* mRNA, which encodes an RNA polymerase II large subunit, was used as a normalization control. The primer sequences used for qRT–PCR analysis are as follows: 5′-TGGAACTCTGGAGTCACACC (forward) and 5′-CATCCTCCTTCATTGAACGG (reverse) for *ama-1*, 5′-TGTTAGACAATGCCATGATGAA (forward) and 5′-ATTGGCTGTGCAGTTGTACC (reverse) for *T24B8.5*, 5′-GAACAATAGTGTCAAGCCGATCTGC (forward) and 5′-TTCTGAATGATGAATGCATGTTTAC (reverse) for *C17H12.8*[†], 5′-TCTGGTCAAAATATCCTCCGGGAAG (forward) and 5′-GAGCATCACTCGATTGATTGCAGTG (reverse) for *K08D8.5*, 5′-GTTCAAAAGGACTTAAAGGTCGTTC (forward) and 5′-GGGAATACACTTTTCCTTGAGCCTC (reverse) for *hsp-6*, 5′-CTATGGGCCCAAAAGGAAGAAACGTG (forward) and 5′-GGATTTCGCGACGGTGACTCCGTCC (reverse) for *hsp-60*.

Generation of transgenic animals

To generate translational *hsp-60p::hsp-60::GFP* fusion construct, *hsp-60* cDNA fragment (*hsp-60cDNA*) amplified from *C. elegans* cDNA was PCR-fused with a 2 kb *hsp-60* promoter fragment (*hsp-60p*) amplified from *C. elegans* genomic DNA. XbaI and XmaI sites were used to insert the *hsp-60p::hsp-60cDNA* fragment into a *GFP*-containing pPD95.75 vector. Translational *hsp-60p::hsp-60cDNA* without a tag was generated by performing site-directed mutagenesis to remove GFP from the *hsp-60p::hsp-60::GFP*-containing vector. Only two different lines of transgenic *hsp-60p::hsp-60cDNA* animals, which displayed slight induction of *hsp-60* (Fig EV5B), were obtained over 150 microinjected animals with a low concentration of DNA (5 ng/μl). We therefore speculate that too high level of *hsp-60* may be toxic, and that may be the reason why obtaining *hsp-60*-overexpressing animals was difficult. To generate *hsp-60p::GFP^{MT}* construct, the 2 kb *hsp-60* promoter and the N-terminal mitochondrial targeting sequence (MTS, predicted by MitoProt II)

(Claros & Vincens, 1996) of *hsp-60* amplified from *C. elegans* genomic DNA was inserted into pPD95.75 vector by using EZ fusion™ cloning method (Enzynomics, Daejeon, Korea). The resulting plasmids containing *hsp-60p::hsp-60cDNA::GFP* (5 ng/μl), *hsp-60::hsp-60cDNA* (5 ng/μl), or *hsp-60p::GFP^{MT}* (5 ng/μl) were co-injected with an injection marker *odr-1p::RFP* (75 ng/μl) into the gonad of young (day 1) adult wild-type worms. To generate *vha-6p::tagRFP* transcriptional fusion construct, *GFP* in pPD95.75 was replaced by *tagRFP* amplified from PSD-95-pTagRFP, a gift from Johannes Hell (Addgene plasmid # 52671), by using the EZ fusion™ cloning method. A PCR-amplified 850 bp *vha-6* promoter fragment was inserted into the *tagRFP*-containing pPD95.75 (pIJ559) by using the EZ fusion™ cloning method. To generate *vha-6p::pmk-1::tagRFP* and *vha-6p::sek-1::tagRFP* translational fusion constructs, *pmk-1* and *sek-1* cDNAs were PCR-amplified from *C. elegans* cDNA samples and inserted into the *tagRFP*-containing pPD95.75 (pIJ559) by using the EZ fusion™ cloning method. Subsequently, the 850 bp *vha-6* promoter fragment was inserted into *pmk-1::tagRFP*- or *sek-1::tagRFP*-containing plasmids by using the EZ fusion™ cloning method. The resulting plasmids that contain *vha-6p::tagRFP* (25 ng/μl), *vha-6p::pmk-1::tagRFP* (25 ng/μl), or *vha-6p::sek-1::tagRFP* (25 ng/μl) were injected with the co-injection marker *ofm-1p::GFP* (75 ng/μl) into the gonad of day 1 adult wild-type worms. To generate intestine-specific *hsp-60::tagRFP* construct, *pmk-1* cDNA in the *vha-6p::pmk-1::tagRFP*-containing vector was replaced by *hsp-60* cDNA by using the EZ fusion™ method. *vha-6* promoter in the resulting plasmid was further replaced by *unc-119* promoter for neuron-specific *hsp-60::tagRFP* construct. Intestinal and neuronal *hsp-60::tagRFP* translational fusion constructs (5 ng/μl) were injected with co-injection markers, *odr-1p::RFP* (75 ng/μl) and *fasn-1p::GFP* (75 ng/μl), respectively. To generate *hsp-60::spGFPN* and *sek-1::spGFPC* constructs, *tagRFP* in the *vha-6p::hsp-60::tagRFP*- and *vha-6p::sek-1::tagRFP*-containing vectors was replaced by *spGFPN* and *spGFPC*, respectively, by using the EZ fusion™ method. *sek-1* cDNA in the *vha-6p::sek-1::tagRFP*-containing vector was replaced by *Y22D7AL.10* cDNA by using the EZ fusion™ method to generate *vha-6p::Y22D7AL.10::spGFPC* construct. To generate *vha-6p::spGFPC* construct, *tagRFP* in the *vha-6p::tagRFP*-containing vector was replaced by *spGFPC* by using the EZ fusion™ method. The *vha-6p::hsp-60::spGFPN*-containing vector (5 ng/μl) was injected with the co-injection marker *odr-1p::RFP* (75 ng/μl). Each of the *vha-6p::sek-1::spGFPC* (25 ng/μl)-, *vha-6p::Y22D7AL.10::spGFP* (5 ng/μl)-, or *vha-6p::spGFPC* (25 ng/μl)-containing vectors was injected with the co-injection marker *coel::RFP* (75 ng/μl) into the gonad of day 1 adult worms. The primer sequences used for cloning are as follows: 5′-GTAGTTTTTCAGACACAAAAGATGCTTCGCCTCGCCAGAAAG (forward) 5′-GTACCCCGGGTGAATCCCATTCCTCCCATAC (reverse) for *hsp-60* cDNA, 5′-GCTCTAGAGCCGCGGAAGATTGAGTATTCC (forward) and 5′-ATGCTTCGCCTCGCCAGAAAGCTTTTGTGTCTGAAAAACTAC (reverse) for *hsp-60* promoter, 5′-GAATGGGATTCTAGCATTCGTAGAATTCCAACTGAGCGCCGG (forward) and 5′-CGAATGCTAGAATCCCATTCCTCCCATACCGCCCATTCCAC (reverse) for site-directed mutagenesis to generate *hsp-60p::hsp-60cDNA*, 5′-CTGCAGGTCGACTCTAGACGCGGAAGATTGAGTATTCC (forward) and 5′-CCTTTGGCCAATCCCGGGTTCCCCACGACTGCT

[†]Correction added on 13 April 2017, after first online publication: The gene name *C17H11.8* was corrected to *C17H12.8*.

CGATGATC (reverse) for *hsp-60* promoter-MTS. 5′-GGACCCTTGG AGGGTACCATGGTGTCTAAGGGCGAAGAG (forward) and 5′-GGCG CTCAGTTGGAATTCTCAATTAAGTTTGTGCCCCAGTTTG (reverse) for *tagRFP*, 5′-TGGAAATGAAATAAGCTTAGCACAGAACTGCATTA AG (forward) and 5′-CTTAGACACCATGGTACCTTTTTATGGGTTTT GGTAGG (reverse) for *vha-6* promoter, 5′-CTGCAGGTCGACTCTAG AATGTTTCCACAGACAACAATGG (forward) and CCTTTGGCCAA TCCCGGGATCGATTCCATTTTCTCCTC (reverse) for *pmk-1* cDNA, 5′-GCGCCAGGATACTCTAGAATGGAGCGAAAAGGACGTGAGC (for-ward) and 5′-CCTTTGGCCAATCCCGGGATCGTCGCCAAACAGTGT CGAG (reverse) for *sek-1* cDNA, 5′-TGGAAATGAAATAAGCTTAGC ACAGAACTGCATTAAG (forward) and 5′-CTGTGGAAACATTCTAG ATTTTTATGGGTTTTGGTAGG (reverse) for *vha-6* promoter for *vha-6p::pmk-1::tagRFP*, 5′-TGGAAATGAAATAAGCTTAGCACAGAA CTGCATTAAG (forward) and 5′-TTTTCGCTCCATTCTAGATTTTTA TGGGTTTTGGTAGG (reverse) for *vha-6* promoter for *vha-6p::sek-1::tagRFP*, 5′-AACCCATAAAAATCTAGAATGCTTCGCCTCGCCAGA AAG (forward) and 5′- CCTTTGGCCAATCCCGGGATGAATCCCATT CCTCCCATAC (reverse) for *hsp-60* cDNA for *vha-6p::hsp-60:: tagRFP*, 5′-GATTCATTAATGCAGCTGGTGTCAAGTCTCTCAAAATT C (forward) and 5′-GAGGCGAAGCATTCTAGAATATGCTGTTGTAG CTGAAAATTTG (reverse) for *unc-119* promoter for *unc-119p::hsp-60::tagRFP*, 5′-GGACCCTTGGAGGGTACCATGTCCAAAGGAGAA-GAAC (forward) and 5′-GGCGCTCAGTTGGAATTCTTATGTTCCTTT TTCATTTGG (reverse) for *spGFPN* for *vha-6p::hsp-60::spGFPN*, 5′-G GACCCTTGGAGGGTACCAGAGATCATATGGTGTTG (forward) and 5′-GGCGCTCAGTTGGAATTCTTATCCAGTAATACCTGCAGC (reverse) for *spGFPC* for *vha-6p::sek-1::spGFPC*, 5′-AACCCATAAAAATCTAG AATGTTCCTCACCGCTGTCC (forward) and 5′-CCTTTGGCCAATCC CGGGATATGGAAGACTCCGAGAAGATC (reverse) for *Y22D7AL.10* cDNA for *vha-6p::Y22D7AL.10::spGFPC*, 5′-AACCCATAAAAAGGTA CCATGAGAGATCATATGGTGTTG (forward) and 5′-GGCGCTCAGT TGGAATTCTTATCCAGTAATACCTGCAGC (reverse) for *spGFPC* for *vha-6p::spGFPC*.

Expanded View for this article is available online.

Acknowledgements

Author contributions

Conflict of interest

The authors declare that they have no conflict of interest.

References

Amberger A, Maczek C, Jurgens G, Michaelis D, Schett G, Trieb K, Eberl T, Jindal S, Xu Q, Wick G (1997) Co-expression of ICAM-1, VCAM-1, ELAM-1 and Hsp60 in human arterial and venous endothelial cells in response to cytokines and oxidized low-density lipoproteins. *Cell Stress Chaperones* 2: 94 – 103

Ashburner M, Ball CA, Blake JA, Botstein D, Butler H, Cherry JM, Davis AP, Dolinski K, Dwight SS, Eppig JT, Harris MA, Hill DP, Issel-Tarver L, Kasarskis A, Lewis S, Matese JC, Richardson JE, Ringwald M, Rubin GM, Sherlock G (2000) Gene ontology: tool for the unification of biology. The Gene Ontology Consortium. *Nat Genet* 25: 25 – 29

Benedetti C, Haynes CM, Yang Y, Harding HP, Ron D (2006) Ubiquitin-like protein 5 positively regulates chaperone gene expression in the mitochondrial unfolded protein response. *Genetics* 174: 229 – 239

Bolz DD, Tenor JL, Aballay A (2010) A conserved PMK-1/p38 MAPK is required in *Caenorhabditis elegans* tissue-specific immune response to *Yersinia pestis* infection. *J Biol Chem* 285: 10832 – 10840

Bukau B, Horwich AL (1998) The Hsp70 and Hsp60 chaperone machines. *Cell* 92: 351 – 366

Calixto A, Chelur D, Topalidou I, Chen X, Chalfie M (2010) Enhanced neuronal RNAi in *C. elegans* using SID-1. *Nat Methods* 7: 554 – 559

Cappello F, Conway de Macario E, Marasa L, Zummo G, Macario AJ (2008) Hsp60 expression, new locations, functions and perspectives for cancer diagnosis and therapy. *Cancer Biol Ther* 7: 801 – 809

Chen D, Pan KZ, Palter JE, Kapahi P (2007) Longevity determined by developmental arrest genes in Caenorhabditis elegans. *Aging Cell* 6: 525 – 533

Chen W, Syldath U, Bellmann K, Burkart V, Kolb H (1999) Human 60-kDa heat-shock protein: a danger signal to the innate immune system. *J Immunol* 162: 3212 – 3219

Chikka MR, Anbalagan C, Dvorak K, Dombeck K, Prahlad V (2016) The mitochondria-regulated immune pathway activated in the *C. elegans* intestine is neuroprotective. *Cell Rep* 16: 2399 – 2414

Chun JN, Choi B, Lee KW, Lee DJ, Kang DH, Lee JY, Song IS, Kim HI, Lee SH, Kim HS, Lee NK, Lee SY, Lee KJ, Kim J, Kang SW (2010) Cytosolic Hsp60 is involved in the NF-kappaB-dependent survival of cancer cells via IKK regulation. *PLoS One* 5: e9422

Claros MG, Vincens P (1996) Computational method to predict mitochondrially imported proteins and their targeting sequences. *Eur J Biochem* 241: 779 – 786

Couillault C, Pujol N, Reboul J, Sabatier L, Guichou JF, Kohara Y, Ewbank JJ (2004) TLR-independent control of innate immunity in *Caenorhabditis elegans* by the TIR domain adaptor protein TIR-1, an ortholog of human SARM. *Nat Immunol* 5: 488 – 494

Curran SP, Ruvkun G (2007) Lifespan regulation by evolutionarily conserved genes essential for viability. *PLoS Genet* 3: e56

Estes KA, Dunbar TL, Powell JR, Ausubel FM, Troemel ER (2010) bZIP transcription factor *zip-2* mediates an early response to *Pseudomonas aeruginosa* infection in *Caenorhabditis elegans*. *Proc Natl Acad Sci USA* 107: 2153 – 2158

Evans EA, Kawli T, Tan MW (2008) *Pseudomonas aeruginosa* suppresses host immunity by activating the DAF-2 insulin-like signaling pathway in *Caenorhabditis elegans*. *PLoS Pathog* 4: e1000175

Ewbank JJ (2006) Signaling in the immune response. In *The C. elegans Research Community, WormBook*. WormBook (ed). doi: 10.1895/wormbook. 1.83.1, http://www.wormbook.org

Ewbank JJ, Pujol N (2016) Local and long-range activation of innate immunity by infection and damage in *C. elegans*. *Curr Opin Immunol* 38: 1 – 7

Fares H, Greenwald I (2001) Genetic analysis of endocytosis in *Caenorhabditis elegans*: coelomocyte uptake defective mutants. *Genetics* 159: 133–145

Feinberg EH, Vanhoven MK, Bendesky A, Wang G, Fetter RD, Shen K, Bargmann CI (2008) GFP Reconstitution Across Synaptic Partners (GRASP) defines cell contacts and synapses in living nervous systems. *Neuron* 57: 353–363

Gaglia MM, Jeong DE, Ryu EA, Lee D, Kenyon C, Lee SJ (2012) Genes that act downstream of sensory neurons to influence longevity, dauer formation, and pathogen responses in *Caenorhabditis elegans*. *PLoS Genet* 8: e1003133

Gao B, Tsan MF (2003) Recombinant human heat shock protein 60 does not induce the release of tumor necrosis factor alpha from murine macrophages. *J Biol Chem* 278: 22523–22529

Garsin DA, Sifri CD, Mylonakis E, Qin X, Singh KV, Murray BE, Calderwood SB, Ausubel FM (2001) A simple model host for identifying Gram-positive virulence factors. *Proc Natl Acad Sci USA* 98: 10892–10897

Garsin DA, Villanueva JM, Begun J, Kim DH, Sifri CD, Calderwood SB, Ruvkun G, Ausubel FM (2003) Long-lived *C. elegans daf-2* mutants are resistant to bacterial pathogens. *Science* 300: 1921

Gene Ontology Consortium (2015) Gene Ontology Consortium: going forward. *Nucleic Acids Res* 43: D1049–D1056

Ghosh I, Hamilton AD, Regan L (2000) Antiparallel leucine zipper-directed protein reassembly: application to the green fluorescent protein. *J Am Chem Soc* 122: 5568–5569

Gibson TJ, Seiler M, Veitia RA (2013) The transience of transient overexpression. *Nat Methods* 10: 715–721

Govindan JA, Jayamani E, Zhang X, Mylonakis E, Ruvkun G (2015) Dialogue between *E. coli* free radical pathways and the mitochondria of *C. elegans*. *Proc Natl Acad Sci USA* 112: 12456–12461

Gupta S, Knowlton AA (2007) HSP60 trafficking in adult cardiac myocytes: role of the exosomal pathway. *Am J Physiol Heart Circ Physiol* 292: H3052–H3056

Habich C, Kempe K, van der Zee R, Rumenapf R, Akiyama H, Kolb H, Burkart V (2005) Heat shock protein 60: specific binding of lipopolysaccharide. *J Immunol* 174: 1298–1305

Haynes CM, Petrova K, Benedetti C, Yang Y, Ron D (2007) ClpP mediates activation of a mitochondrial unfolded protein response in *C. elegans*. *Dev Cell* 13: 467–480

Haynes CM, Yang Y, Blais SP, Neubert TA, Ron D (2010) The matrix peptide exporter HAF-1 signals a mitochondrial UPR by activating the transcription factor ZC376.7 in *C. elegans*. *Mol Cell* 37: 529–540

Hiatt SM, Shyu YJ, Duren HM, Hu CD (2008) Bimolecular fluorescence complementation (BiFC) analysis of protein interactions in *Caenorhabditis elegans*. *Methods* 45: 185–191

Honda Y, Honda S (1999) The *daf-2* gene network for longevity regulates oxidative stress resistance and Mn-superoxide dismutase gene expression in *Caenorhabditis elegans*. *FASEB J* 13: 1385–1393

de Hoon MJ, Imoto S, Nolan J, Miyano S (2004) Open source clustering software. *Bioinformatics* 20: 1453–1454

Hu CD, Chinenov Y, Kerppola TK (2002) Visualization of interactions among bZIP and Rel family proteins in living cells using bimolecular fluorescence complementation. *Mol Cell* 9: 789–798

Hwang AB, Ryu EA, Artan M, Chang HW, Kabir MH, Nam HJ, Lee D, Yang JS, Kim S, Mair WB, Lee C, Lee SS, Lee SJ (2014) Feedback regulation via AMPK and HIF-1 mediates ROS-dependent longevity in *Caenorhabditis elegans*. *Proc Natl Acad Sci USA* 111: E4458–E4467

Irazoqui JE, Urbach JM, Ausubel FM (2010) Evolution of host innate defence: insights from *Caenorhabditis elegans* and primitive invertebrates. *Nat Rev Immunol* 10: 47–58

Jonassen T, Marbois BN, Faull KF, Clarke CF, Larsen PL (2002) Development and fertility in *Caenorhabditis elegans clk-1* mutants depend upon transport of dietary coenzyme Q8 to mitochondria. *J Biol Chem* 277: 45020–45027

Kahn NW, Rea SL, Moyle S, Kell A, Johnson TE (2008) Proteasomal dysfunction activates the transcription factor SKN-1 and produces a selective oxidative-stress response in *Caenorhabditis elegans*. *Biochem J* 409: 205–213

Kalderon B, Kogan G, Bubis E, Pines O (2015) Cytosolic Hsp60 can modulate proteasome activity in yeast. *J Biol Chem* 290: 3542–3551

Kim DH, Feinbaum R, Alloing G, Emerson FE, Garsin DA, Inoue H, Tanaka-Hino M, Hisamoto N, Matsumoto K, Tan MW, Ausubel FM (2002) A conserved p38 MAP kinase pathway in *Caenorhabditis elegans* innate immunity. *Science* 297: 623–626

Kim DH, Liberati NT, Mizuno T, Inoue H, Hisamoto N, Matsumoto K, Ausubel FM (2004) Integration of *Caenorhabditis elegans* MAPK pathways mediating immunity and stress resistance by MEK-1 MAPK kinase and VHP-1 MAPK phosphatase. *Proc Natl Acad Sci USA* 101: 10990–10994

Kim DH (2013) Bacteria and the aging and longevity of *Caenorhabditis elegans*. *Annu Rev Genet* 47: 233–246

Kim DH, Ewbank JJ (2015) Signaling in the innate immune response. In *The C. elegans Research Community, WormBook*. WormBook (ed). doi: 10.1895/wormbook.1.83.2, http://www.wormbook.org

Kirienko NV, Ausubel FM, Ruvkun G (2015) Mitophagy confers resistance to siderophore-mediated killing by *Pseudomonas aeruginosa*. *Proc Natl Acad Sci USA* 112: 1821–1826

Kol A, Lichtman AH, Finberg RW, Libby P, Kurt-Jones EA (2000) Cutting edge: heat shock protein (HSP) 60 activates the innate immune response: CD14 is an essential receptor for HSP60 activation of mononuclear cells. *J Immunol* 164: 13–17

Lee D, Jeong DE, Son HG, Yamaoka Y, Kim H, Seo K, Khan AA, Roh TY, Moon DW, Lee Y, Lee SJ (2015) SREBP and MDT-15 protect *C. elegans* from glucose-induced accelerated aging by preventing accumulation of saturated fat. *Genes Dev* 29: 2490–2503

Liberati NT, Fitzgerald KA, Kim DH, Feinbaum R, Golenbock DT, Ausubel FM (2004) Requirement for a conserved Toll/interleukin-1 resistance domain protein in the *Caenorhabditis elegans* immune response. *Proc Natl Acad Sci USA* 101: 6593–6598

Libina N, Berman JR, Kenyon C (2003) Tissue-specific activities of *C. elegans* DAF-16 in the regulation of lifespan. *Cell* 115: 489–502

Lin L, Pan S, Zhao J, Liu C, Wang P, Fu L, Xu X, Jin M, Zhang A (2014) HSPD1 interacts with IRF3 to facilitate interferon-beta induction. *PLoS One* 9: e114874

Liu Y, Samuel BS, Breen PC, Ruvkun G (2014) *Caenorhabditis elegans* pathways that surveil and defend mitochondria. *Nature* 508: 406–410

Merkwirth C, Jovaisaite V, Durieux J, Matilainen O, Jordan SD, Quiros PM, Steffen KK, Williams EG, Mouchiroud L, Tronnes SU, Murillo V, Wolff SC, Shaw RJ, Auwerx J, Dillin A (2016) Two conserved histone demethylases regulate mitochondrial stress-induced longevity. *Cell* 165: 1209–1223

Miyata S, Begun J, Troemel ER, Ausubel FM (2008) DAF-16-dependent suppression of immunity during reproduction in *Caenorhabditis elegans*. *Genetics* 178: 903–918

Nargund AM, Pellegrino MW, Fiorese CJ, Baker BM, Haynes CM (2012) Mitochondrial import efficiency of ATFS-1 regulates mitochondrial UPR activation. *Science* 337: 587–590

Ohashi K, Burkart V, Flohe S, Kolb H (2000) Cutting edge: heat shock protein 60 is a putative endogenous ligand of the toll-like receptor-4 complex. *J Immunol* 164: 558 – 561

O'Neill LA, Golenbock D, Bowie AG (2013) The history of Toll-like receptors - redefining innate immunity. *Nat Rev Immunol* 13: 453 – 460

Pagliarini DJ, Calvo SE, Chang B, Sheth SA, Vafai SB, Ong SE, Walford GA, Sugiana C, Boneh A, Chen WK, Hill DE, Vidal M, Evans JG, Thorburn DR, Carr SA, Mootha VK (2008) A mitochondrial protein compendium elucidates complex I disease biology. *Cell* 134: 112 – 123

Papp D, Csermely P, Soti C (2012) A role for SKN-1/Nrf in pathogen resistance and immunosenescence in *Caenorhabditis elegans*. *PLoS Pathog* 8: e1002673

Pellegrino MW, Nargund AM, Haynes CM (2013) Signaling the mitochondrial unfolded protein response. *Biochim Biophys Acta* 1833: 410 – 416

Pellegrino MW, Nargund AM, Kirienko NV, Gillis R, Fiorese CJ, Haynes CM (2014) Mitochondrial UPR-regulated innate immunity provides resistance to pathogen infection. *Nature* 516: 414 – 417

Powell JR, Kim DH, Ausubel FM (2009) The G protein-coupled receptor FSHR-1 is required for the *Caenorhabditis elegans* innate immune response. *Proc Natl Acad Sci USA* 106: 2782 – 2787

Pradel E, Zhang Y, Pujol N, Matsuyama T, Bargmann CI, Ewbank JJ (2007) Detection and avoidance of a natural product from the pathogenic bacterium *Serratia marcescens* by *Caenorhabditis elegans*. *Proc Natl Acad Sci USA* 104: 2295 – 2300

Pukkila-Worley R, Ausubel FM (2012) Immune defense mechanisms in the *Caenorhabditis elegans* intestinal epithelium. *Curr Opin Immunol* 24: 3 – 9

Qadota H, Inoue M, Hikita T, Koppen M, Hardin JD, Amano M, Moerman DG, Kaibuchi K (2007) Establishment of a tissue-specific RNAi system in *C. elegans*. *Gene* 400: 166 – 173

Quintana FJ, Cohen IR (2011) The HSP60 immune system network. *Trends Immunol* 32: 89 – 95

Reddy KC, Andersen EC, Kruglyak L, Kim DH (2009) A polymorphism in *npr-1* is a behavioral determinant of pathogen susceptibility in *C. elegans*. *Science* 323: 382 – 384

Ren M, Feng H, Fu Y, Land M, Rubin CS (2009) Protein kinase D is an essential regulator of *C. elegans* innate immunity. *Immunity* 30: 521 – 532

Richardson CE, Kooistra T, Kim DH (2010) An essential role for XBP-1 in host protection against immune activation in *C. elegans*. *Nature* 463: 1092 – 1095

Seo M, Seo K, Hwang W, Koo HJ, Hahm JH, Yang JS, Han SK, Hwang D, Kim S, Jang SK, Lee Y, Nam HG, Lee SJ (2015) RNA helicase HEL-1 promotes longevity by specifically activating DAF-16/FOXO transcription factor signaling in *Caenorhabditis elegans*. *Proc Natl Acad Sci USA* 112: E4246 – E4255

Shivers RP, Kooistra T, Chu SW, Pagano DJ, Kim DH (2009) Tissue-specific activities of an immune signaling module regulate physiological responses to pathogenic and nutritional bacteria in *C. elegans*. *Cell Host Microbe* 6: 321 – 330

Shivers RP, Pagano DJ, Kooistra T, Richardson CE, Reddy KC, Whitney JK, Kamanzi O, Matsumoto K, Hisamoto N, Kim DH (2010) Phosphorylation of the conserved transcription factor ATF-7 by PMK-1 p38 MAPK regulates innate immunity in *Caenorhabditis elegans*. *PLoS Genet* 6: e1000892

Shyu YJ, Hiatt SM, Duren HM, Ellis RE, Kerppola TK, Hu CD (2008) Visualization of protein interactions in living *Caenorhabditis elegans* using bimolecular fluorescence complementation analysis. *Nat Protoc* 3: 588 – 596

Soltys BJ, Gupta RS (1996) Immunoelectron microscopic localization of the 60-kDa heat shock chaperonin protein (Hsp60) in mammalian cells. *Exp Cell Res* 222: 16 – 27

Stiernagle T (2006) Maintenance of *C. elegans*. In *The C. elegans Research Community, WormBook*. WormBook (ed). doi: 10.1895/wormbook.1.101.1, http://www.wormbook.org

Swaroop S, Sengupta N, Suryawanshi AR, Adlakha YK, Basu A (2016) HSP60 plays a regulatory role in IL-1beta-induced microglial inflammation via TLR4-p38 MAPK axis. *J Neuroinflammation* 13: 27

Tan MW, Mahajan-Miklos S, Ausubel FM (1999) Killing of *Caenorhabditis elegans* by *Pseudomonas aeruginosa* used to model mammalian bacterial pathogenesis. *Proc Natl Acad Sci USA* 96: 715 – 720

Tian Y, Garcia G, Bian Q, Steffen KK, Joe L, Wolff S, Meyer BJ, Dillin A (2016) Mitochondrial stress induces chromatin reorganization to promote longevity and UPR^{mt}. *Cell* 165: 1197 – 1208

Troemel ER, Chu SW, Reinke V, Lee SS, Ausubel FM, Kim DH (2006) p38 MAPK regulates expression of immune response genes and contributes to longevity in *C. elegans*. *PLoS Genet* 2: e183

Tsan MF, Gao B (2009) Heat shock proteins and immune system. *J Leukoc Biol* 85: 905 – 910

West AP, Shadel GS, Ghosh S (2011) Mitochondria in innate immune responses. *Nat Rev Immunol* 11: 389 – 402

Xie Y, Moussaif M, Choi S, Xu L, Sze JY (2013) RFX transcription factor DAF-19 regulates 5-HT and innate immune responses to pathogenic bacteria in *Caenorhabditis elegans*. *PLoS Genet* 9: e1003324

Yang JS, Nam HJ, Seo M, Han SK, Choi Y, Nam HG, Lee SJ, Kim S (2011) OASIS: online application for the survival analysis of lifespan assays performed in aging research. *PLoS One* 6: e23525

Yoneda T, Benedetti C, Urano F, Clark SG, Harding HP, Ron D (2004) Compartment-specific perturbation of protein handling activates genes encoding mitochondrial chaperones. *J Cell Sci* 117: 4055 – 4066

Zhang S, Ma C, Chalfie M (2004) Combinatorial marking of cells and organelles with reconstituted fluorescent proteins. *Cell* 119: 137 – 144